Deep-Sea Research I 86 (2014) 39–55

Contents lists available at ScienceDirect

Deep-Sea Research I

journal homepage: www.elsevier.com/locate/dsri

# The Arctic Ocean carbon sink

G.A. MacGilchrist [a,*], A.C. Naveira Garabato [a], T. Tsubouchi [b], S. Bacon [b], S. Torres-Valdés [b], K. Azetsu-Scott [c]

[a] University of Southampton, Southampton, UK
[b] National Oceanography Centre, Southampton, Southampton, UK
[c] Ocean Sciences Division, Department of Fisheries and Oceans, Bedford Institute of Oceanography, Dartmouth, NS, Canada

ARTICLE INFO

*Article history:*
Received 21 May 2013
Received in revised form
8 November 2013
Accepted 7 January 2014
Available online 18 January 2014

*Keywords:*
Arctic Ocean
Dissolved inorganic carbon
Carbon budget
Air–sea carbon dioxide flux
Carbon sequestration
Biological pump

ABSTRACT

We present observation based estimates of the transport of dissolved inorganic carbon (DIC) across the four main Arctic Ocean gateways (Davis Strait, Fram Strait, Barents Sea Opening and Bering Strait). Combining a recently derived velocity field at these boundaries with measurements of DIC, we calculated a net summertime pan-Arctic export of $231 \pm 49$ Tg C $yr^{-1}$. On an annual basis, we estimate that at least $166 \pm 60$ Tg C $yr^{-1}$ of this is due to uptake of $CO_2$ from the atmosphere, although time-dependent changes in carbon storage are not quantified. To further understand the region's role as a carbon sink, we calculated the volume-conserved net DIC transport from beneath a prescribed mixed layer depth of 50 m, referred to as 'interior transport', revealing an export of $61 \pm 23$ Tg C $yr^{-1}$. Applying a carbon framework to infer the sources of interior transport implied that this export is primarily due to the sinking and remineralisation of organic matter, highlighting the importance of the biological pump. Furthermore, we qualitatively show that the present day Arctic Ocean is accumulating anthropogenic carbon beneath the mixed layer, imported in Atlantic Water.



## 1. Introduction

The fate of the Arctic Ocean carbon cycle in the face of rapid climate change is of global importance. Observations suggest that despite extensive ice coverage, the Arctic Ocean presently acts as a sink for atmospheric $CO_2$ and even plays a disproportionate role in global oceanic uptake, relative to its surface area (Bates and Mathis, 2009). High levels of primary production over extensive shelf seas (Fransson et al., 2001; Kaltin and Anderson, 2005), surface water cooling (Kaltin et al., 2002; Murata and Takizawa, 2003), and sea–ice dynamics (Anderson et al., 2004; Rysgaard et al., 2007; Else et al., 2011) have all been observed to induce locally significant $CO_2$ uptake. These processes are already undergoing measurable change as a consequence of regional warming (Bates et al., 2006; Arrigo et al., 2008; Lalande et al., 2009a; Cai et al., 2010; Brown and Arrigo, 2012), while further changes such as greater wind-induced mixing (Mathis et al., 2012) and higher inputs of terrigenous organic matter (McGuire et al., 2009) perturb the region's carbon cycle in unquantified ways. As such, opinion remains divided on what will be the net effect of environmental change on the Arctic Ocean $CO_2$ sink (Cai et al., 2010; Jutterström and Anderson, 2010; Else et al., 2013b).

In spite of its global importance and the likelihood of significant change, the Arctic Ocean carbon cycle remains poorly quantified. The spatial and temporal variability of the carbon system means that localised, largely summertime measurements are not easily extrapolated to wider regions or long timescales. This is particularly true of important parameters such as surface water $pCO_2$ (e.g. Fransson et al., 2009) and vertical export of organic carbon out of the mixed layer (e.g. Lalande et al., 2009b). Consequently, most research remains regional, while little is understood about processes on a pan-Arctic scale.

Appreciation for the importance of the Arctic Ocean has resulted in increased effort to understand the pan-Arctic carbon budget. A comprehensive sampling strategy has led to more accurate estimates of annual river inputs (Holmes et al., 2012; Tank et al., 2012) while year-round measurement of coastal ice-covered regions has improved understanding of the role of polynyas in $CO_2$ uptake (Else et al., 2011, 2013a) and satellites are increasingly invoked to understand phytoplankton bloom dynamics (Perrette et al., 2011) and quantify primary production (Brown and Arrigo, 2012). Nevertheless, attempts to quantify pan-Arctic $CO_2$ uptake remain inhibited by a lack of measurements to constrain budget estimates (Lundberg and Haugan, 1996; Anderson et al., 1998) or to validate empirical and numerical models (Arrigo et al., 2010; Manizza et al., 2011, 2013). A

* Corresponding author. Present address: Department of Earth Sciences, University of Oxford, Oxford, UK.
*E-mail address:* graeme.macgilchrist@earth.ox.ac.uk (G.A. MacGilchrist).

http://dx.doi.org/10.1016/j.dsr.2014.01.002

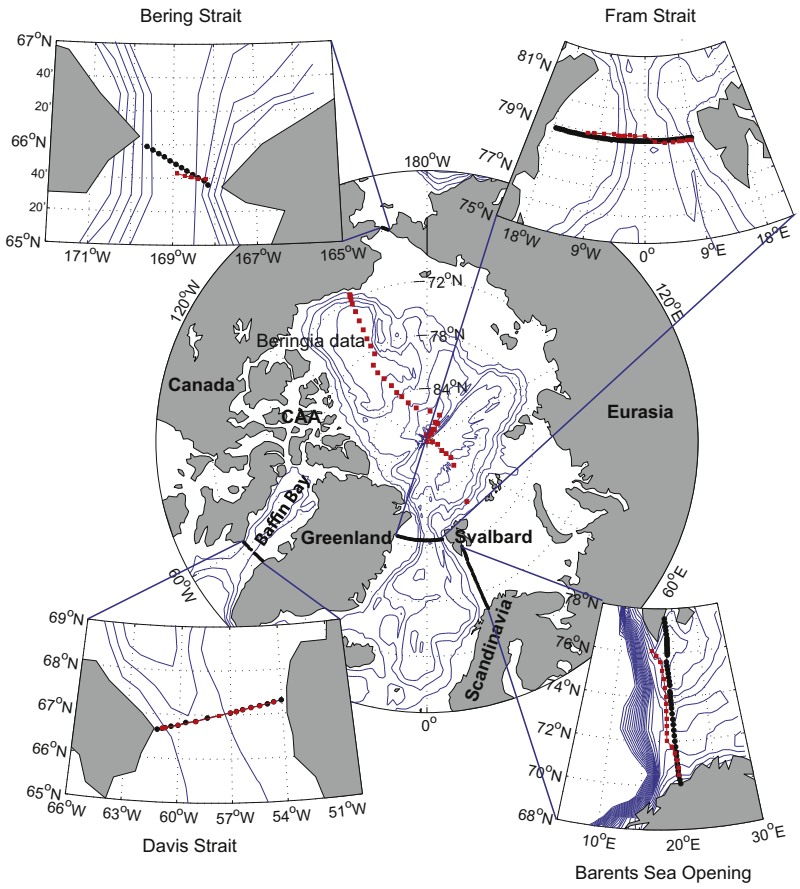


**Fig. 1.** Map of the Arctic Ocean and the four main gateways. Black dots denote the location of CTD stations, while red squares correspond to where carbon data were collected. Measurement stations through the centre of the Arctic are the locations of the Beringia cruise data. CAA stands for Canadian Arctic Archipelago. (For interpretation of the references to colour in this figure caption, the reader is referred to the web version of this paper.)

widespread effort to quantify air–sea $CO_2$ fluxes across the Arctic and North Atlantic concluded that Arctic data are too sparse, and the region too poorly resolved by global models, to make accurate estimates (Schuster et al., 2013).

This study establishes baseline estimates for the transport of dissolved inorganic carbon (DIC) across the main Arctic Ocean boundaries. A recently developed physically consistent velocity field (Tsubouchi et al., 2012; hereafter T2012) across Davis Strait, Fram Strait, Barents Sea Opening (BSO) and Bering Strait (Fig. 1) was combined with measurements of DIC. Net imbalances, across the full depth range and beneath the mixed layer, were then considered in the context of a pan-Arctic DIC budget, allowing complex and variable processes within the Arctic Ocean to be estimated from comparatively simple boundary observations.

The structure of the paper is as follows: Section 2 outlines the methodology, including a derivation of the Arctic Ocean DIC budget and a summary of the carbon framework used to interpret interior transports; results of the carbon framework and transport calculations are presented in Section 3 and discussed in Section 4; conclusions are drawn in Section 5.

## 2. Methods

Transports across the main Arctic Ocean gateways are derived by combining a velocity field with measurements of DIC (throughout this paper, the notation DIC refers to concentration, unless specified otherwise). The velocity field of T2012 is a best-estimate for the summer of 2005, while measurements of DIC were taken from as close to this time as possible (Sections 2.2 and 2.3). As such, the primary results of this study are representative summertime transports. In a further step, we assume these to be representative of annual transport, enabling comparison with previously established terms in the Arctic Ocean DIC budget. We appropriately deal with the uncertainty of this assumption in Section 2.5.

### 2.1. Arctic Ocean DIC budget

The four main gateways enclose the Arctic Ocean in a box (Fig. 1). Conservation of DIC requires that net transport across these gateways, including DIC transported in sea–ice, is balanced by processes occurring within the boundary. These processes comprise changes in the DIC inventory of the ocean over time (i.e. storage), transformation of DIC into other forms of carbon (organic carbon and particulate inorganic carbon) and surface fluxes. This can be written as

$$\int\int_{bot}^{0} vDIC\, dx\, dz = \frac{\partial}{\partial t}\int_{V} DIC\, dV - T - F_s^{DIC} \quad (1)$$

where $v$ is the water velocity normal to the gateway, $DIC$ is the concentration of DIC at the gateways, $V$ is the enclosed volume of the Arctic Ocean, $x$ is the along section dimension, $z$ is the depth, $dV$ is the volume element, $T$ is the net transformation and $F_s^{DIC}$ is the surface flux term, composed of freshwater input ($F_{FW}^{DIC}$) and air–sea gas exchange ($F_{AS}^{DIC}$). The summertime flux of DIC at the gateways was evaluated using the velocity field from the inverse model of T2012 (Section 2.2) and measurements of DIC from the CARINA dataset (Section 2.3). Integrating this vertically from the bottom of the water column ($bot$) to the surface ($z=0$) and horizontally across the width of all four gateways gives net

full-depth transport of DIC from the Arctic Ocean. Note that in this and subsequent equations in which there is a double integral along $dx\,dz$ (i.e. horizontally across gateways and vertical through the water column) limits in $x$ are not displayed, but are always around the full, closed boundary.

The upper water column in the Arctic Ocean has a strong seasonal cycle in DIC that is primarily the result of biological activity, but is also influenced by air–sea gas exchange, river inputs and sea–ice melt and formation. Consequently, synopticity of DIC measurements is an important factor in transport calculations. For our calculations we used the most appropriate data that are publicly available, however the measurements are asynoptic and the uncertainty resulting from this must be considered in relation to full depth transport estimates (Section 2.5). At greater depths, nominally beneath the mixed layer, the seasonality of DIC is dampened or absent, meaning that measurement asynopticity is less of an issue. This has been observed in the Norwegian Sea at Ocean Weather Station M where, between 2001 and 2007, a strong seasonal cycle of DIC was observed in the upper 50 m but no equivalent signal existed below 100 m (Skjelvan et al., 2008).

In addition to transport across the full depth range, net transport of DIC from beneath the mixed layer, hereafter referred to as 'interior transport', was considered. DIC transported in this range is removed from immediate contact with the atmosphere. Thus with careful consideration, interior transport can reveal the extent to which $CO_2$ taken up from the atmosphere is transported beneath the mixed layer, relating it to carbon sequestration and improving understanding of the Arctic Ocean carbon sink. To achieve this we apply a carbon framework that infers the sources of DIC (Section 2.4), and again consider net transports within a carbon budget.

To derive a conservation equation for interior transport, the Arctic Ocean box is separated into a surface and interior layer by the base of the mixed layer (Fig. 2), and the terms in Eq. (1) are split accordingly. Gathering everything on the left hand side and collecting terms relating to the surface and interior boxes gives

$$\left\{\iint_{mld}^{0} vDIC\,dx\,dz + F_s^{DIC} + T_{surf} - \frac{\partial}{\partial t}\int_{surfV} DIC\,dV\right\} + \left\{\iint_{bot}^{mld} vDIC\,dx\,dz + T_{int} - \frac{\partial}{\partial t}\int_{intV} DIC\,dV\right\} = 0 \tag{2}$$

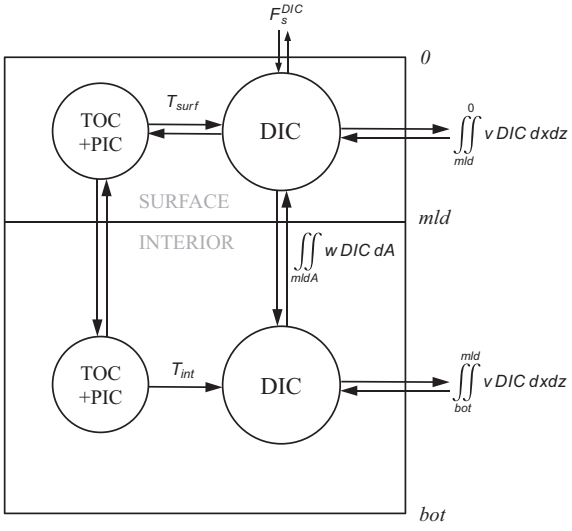


**Fig. 2.** Schematic of two layer ocean showing transport terms associated with the Arctic Ocean DIC budget. See Eqs. (2) and (3) for definition of transport terms and variables. TOC – total organic carbon (dissolved and particulate); PIC – particulate inorganic carbon.

where $mld$ is the mixed layer depth, $T_{surf}$ and $T_{int}$ are the net transformation terms in the surface and interior box respectively and $surfV$ and $intV$ are the enclosed volumes of the surface and interior boxes respectively. The first four terms in Eq. (2) define DIC in the surface box. If the sum of these is non-zero, conservation of DIC requires that the imbalance moves vertically across the mixed layer, into the interior box. This can be written as

$$\iint_{mld}^{0} vDIC\,dx\,dz + F_{surf}^{DIC} + T_{surf} - \frac{\partial}{\partial t}\int_{surfV} DIC\,dV = -\iint_{mldA} wDIC\,dA \tag{3}$$

where $mldA$ is the surface area of the Arctic Ocean at the mixed layer depth, $w$ is the vertical component of water velocity defined such that upward is positive and $dA$ is the horizontal surface area element. Note that this step is only valid because the path of the horizontal boundary integrals is closed and thus DIC cannot be transported anywhere except vertically.

For the vertical flux of DIC across the mixed layer base, velocity and DIC concentration can be defined as the mean value (overbar) at this depth plus a perturbation (prime) from the mean, i.e. $w = \overline{w} + w'$ and $DIC = \overline{DIC} + DIC'$. Applying this to the vertical flux term in Eq. (3), dropping double integrals and limits for simplicity, gives

$$\begin{aligned}\int wDIC\,dA &= \int (\overline{w}\,\overline{DIC} + w'\,\overline{DIC} + \overline{w}DIC' + w'DIC')\,dA \\ &= \int \overline{w}\,\overline{DIC}\,dA + \int w'DIC'\,dA\end{aligned} \tag{4}$$

where, by construction, $\int w'\,dA = \int DIC'\,dA = 0$. This equation defines the vertical flux of DIC as a mean transport, associated with the net movement of water across the mixed layer base, and an 'eddy' transport, for which there is zero net volume transport but where there may be a correlation between DIC and the direction of vertical motion across the mixed layer base.

The net movement of water across the mixed layer base is equal to the net volume imbalance beneath the mixed layer at the ocean boundaries:

$$\iint_{mldA} \overline{w}\,dA = \iint_{bot}^{mld} v\,dx\,dz \tag{5}$$

Applying this to Eq. (4), the vertical flux term can be redefined as

$$\iint_{mldA} wDIC\,dA = \overline{DIC}\iint_{bot}^{mld} v\,dx\,dz + \iint_{mldA} w'DIC'\,dA \tag{6}$$

Thus, replacing the surface terms in Eq. (2) with the vertical flux given by Eq. (6), an expression for the conservation of DIC beneath the mixed layer is

$$\iint_{bot}^{mld} vDIC\,dx\,dz - \overline{DIC}\iint_{bot}^{mld} v\,dx\,dz = \frac{\partial}{\partial t}\int_{intV} DIC\,dV - T_{int} + \int w'DIC'\,dA \tag{7}$$

where the left hand side is what we define as interior transport. This definition preserves volume conservation for the interior box and allows net interior transport to be related to processes occurring within the Arctic Ocean boundaries. Thus, Eq. (7) states that net interior transport of DIC is controlled by three processes: the change in DIC storage over time, the net transformation of DIC between other forms of carbon and the 'eddy' contribution of vertical transport. These latter two terms represent biological and (volume conserved) physical sequestration of carbon out of the mixed layer, respectively. A schematic of the terms in the two-layer box formulation is presented in Fig. 2.

For the purpose of this calculation, a prescribed mixed layer depth was defined. In most regions of the Arctic Ocean, the mixed layer depth is thought to be between 30 and 50 m (Schlosser et al., 1995). This is supported by the density gradients in this study which are highest around these depths (Fig. 4). In addition, this is the depth range where there is the greatest depletion of DIC

**Table 1**
Data sources for CTD, DIC and $\delta^{18}O$ measurements.

| Data type | Gateway | Location | Date | Number of stations | Reference | Notes |
|---|---|---|---|---|---|---|
| CTD | Davis | Full | Sep 2005 | 16 | Lee et al. (2004) | |
| | Fram | Full | Aug-Sep 2005 | 74 | Fahrbach and Lemke (2005) | |
| | BSO | 70 to 74°N and 76 to 77°N | Aug 2005 | 29 | Skagseth et al. (2008) | |
| | | Missing locations | | 16 | | NEMO GCM |
| | Bering | Full | Aug 2005 | 12 | Woodgate et al. (2008) | |
| DIC | Davis | Full | Sep 2005 | 11 | Azetsu-Scott et al. (2010) | |
| | Fram | West of 0°W | May 2002 | 10 | Anderson (2007) | |
| | | East of 0°W | June 2002 | 7 | Bellerby and Smethie (2007) | |
| | BSO | Full | June 2002 | 18 | Bellerby and Smethie (2007) | |
| | Bering | East of 169°W | July 2004 | 5 | Codispoti and Swift (2007) | |
| | Central Arctic | see Fig. 1 | Aug-Sep 2005 | 48 | Tanhua et al. (2009) | Beringia Cruise |
| DIC (secondary dataset) | Davis | Full | Aug 1997 | 7 | Jones et al. (2007) | |
| | BSO | South of 74°N | Sep 2003 | 8 | Johannessen and Olsen (2007) | |
| | Bering | East of 169°W | July 2002 | 5 | Bates et al. (2007) | |
| $\delta^{18}O$ | Davis | Full | 2005 | 11 | Lee et al. (2004) | |
| | Fram | Full | 1998/2004/2005 | 58 | Rabe et al. (2009) | |
| | BSO | Full | 2000 | 20 | Schmidt et al. (1999) | |
| | Bering | Full | 2004 | 5 | Woodgate et al. (2008) | |

(Fig. 4), presumed to be due to biological activity. Recent observations suggest that the mixed layer in the central basin is shallower, ranging from just 16 m in summer to 24 m in winter (Toole et al., 2010). For the primary results of this study, a mixed layer depth of 50 m was chosen. The transport uncertainty induced by prescribing a fixed mixed layer depth is considered in Section 2.5. It should also be kept in mind throughout this paper that discussion of below mixed layer DIC transport and sequestration are in reference to a fixed depth of 50 m and not the true mixed layer depth. Mean DIC at the mixed layer depth, $\overline{DIC}$, is estimated as the mean of measurements within $\pm 10$ m of this depth, at the ocean gateways and in the central Arctic Ocean.

### 2.2. Velocity field

The velocity field is the inverse model solution of T2012. Geostrophic velocities were determined using hydrographic CTD measurements from the summer of 2005 supplemented by a small quantity of output from a general circulation model, NEMO (see Table 1 for data sources). Reference velocities were determined by moored current meters and ship based ADCP measurements and were adjusted by the inverse model with a priori uncertainties to satisfy mass and salinity conservation constraints within the Arctic Ocean. The resulting velocity field is considered to be representative of the circulation in the summer of 2005. See T2012 for details.

Figure 3 shows the velocity field for the four gateways and the cumulative volume transport evaluated from the west of Davis Strait to the east of Bering Strait, with absolute values for specific regions presented in Table 3. The main inflows to the Arctic Ocean are Atlantic Water entering in the southern half of BSO ($3.4 \pm 0.5$ Sv) and in the West Spitsbergen Current to the east of Fram Strait ($3.8 \pm 0.6$ Sv) as well as Pacific Water entering through Bering Strait ($1.0 \pm 0.1$ Sv). Water leaves the Arctic primarily through the western side of Davis Strait ($-4.0 \pm 0.3$ Sv) and the East Greenland Current at the western side of the deep section in Fram Strait ($-5.0 \pm 0.9$ Sv). Across the Arctic Ocean there is net lateral divergence of $-0.15$ Sv (Table 2), balanced by surface input of freshwater across the Arctic Ocean surface (the net of river runoff, precipitation and evaporation) and to the export of sea ice across Fram Strait (T2012). The minor discrepancy (0.01 Sv) between this divergence and that of T2012 is due to different adopted methods of bottom triangle formulation.

When considering the ocean interior only (below 50 m; dashed line in Fig. 3b), there is a divergence of $-1.29$ Sv due to water sinking from the near-surface ocean. As a result of this volume imbalance, the second term on the left hand side of Eq. (7) is non-zero, and the net transport of DIC from beneath the mixed layer is altered thereby to preserve volume conservation in the ocean interior.

### 2.3. Dissolved inorganic carbon

Dissolved inorganic carbon data, with the exception of Davis Strait, were taken from the publicly accessible CARINA (CARbon dioxide IN the Atlantic ocean) database (Jutterström et al., 2010, see Table 1 for sources of component datasets). To ensure consistency with the velocity field, data from years as close to 2005 as possible were used, with all measurements being from spring/summer (Table 1).

Davis Strait data were obtained in September 2005 and consist of 11 stations across the whole gateway, with 73 measurements of DIC. Fram Strait data came from two different cruises in April (western side) and May (eastern side) of 2002 and, in total, comprise 17 stations and 242 DIC measurements. Data for BSO were collected on the same cruise as for the eastern side of Fram Strait and consist of 18 stations and 127 DIC measurements. Bering Strait data are from July 2004 and consist of 5 stations (44 DIC measurements) covering only the eastern half of the channel. A total of 51 stations and 476 measurements of DIC enclose the Arctic Ocean box. All data were optimally interpolated along isobars (Roemmich, 1983) onto the higher resolution 2005 hydrographic data grid so that they could be combined with the velocity field.

The distribution of DIC across the four gateways is shown in Fig. 4. Concentrations exhibit the characteristic oceanic profile of a positive gradient with depth. The most striking feature is the range of values measured in Davis Strait, where concentrations increase from 2050 μmol $kg^{-1}$ in the surface ocean to greater than 2300 μmol $kg^{-1}$ at depth. This deep concentration is considerably higher than in the intermediate and deep waters of Fram Strait and BSO, where DIC values rarely exceed 2220 μmol $kg^{-1}$. However, surface concentrations are notably higher in these regions, ranging from 2120 to 2200 μmol $kg^{-1}$. Concentrations as low as 1900 μmol $kg^{-1}$ are seen in the surface waters of Bering Strait.

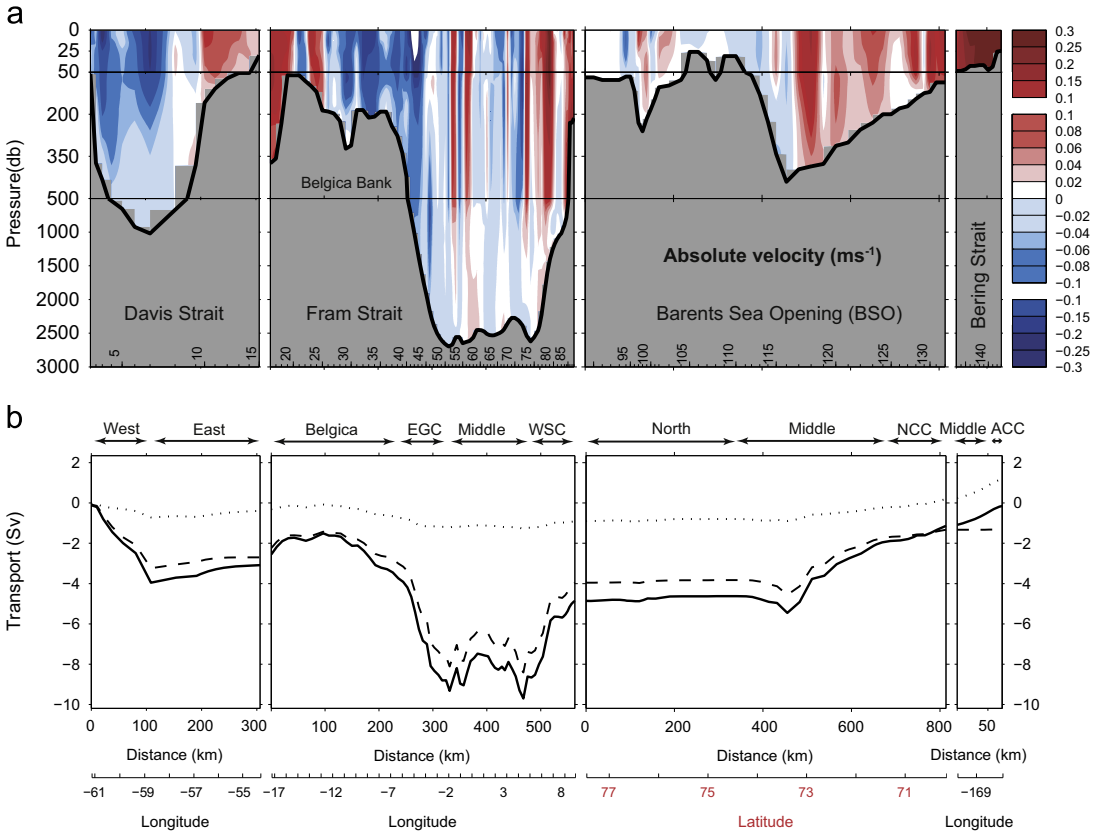


**Fig. 3.** (a) Velocity field across the Arctic Ocean gateways (m $s^{-1}$) and (b) cumulative volume transport from the west of Davis Strait to the east of Bering Strait for the full depth range (solid line), interior (below 50 m; dashed line) and surface layer (above 50 m; dotted line). The width of each gateway is scaled according to its actual width and in (a) depths are expanded between 0 and 50 db and between 50 and 500 db. Abbreviations: EGC (East Greenland Current), WSC (West Spitsbergen Current), NCC (Norwegian Coastal Current) and ACC (Alaskan Coastal Current).

Extrapolation of limited data from the eastern side of Bering Strait across to the western side potentially misrepresents DIC concentrations across this gateway. The 2009 RUSALCA cruise covering the full width of Bering Strait found subsurface DIC values between 150 and 200 μmol $kg^{-1}$ greater in the Russian part of the strait (Bates, pers. comm. 2013). This east–west contrast was also measured in nutrient profiles from 2005 (Chierici and Fransson, 2009; Torres-Valdés et al., 2013) suggesting that it is a persistent feature of Bering Strait. Since we do not have access to full-width Bering Strait data, we maintain the DIC field shown in Fig. 4, but consider the potential bias in our results (Section 3.2.1).

Data for the central Arctic Ocean (from the transpolar Beringia cruise in 2005; Fig. 1) were used in determining $\overline{DIC}$ for interior transport calculations. These consist of 1043 DIC measurements from 48 stations across the Canadian and Eurasian basins (Table 1).

### 2.4. Carbon framework

According to the framework outlined in Williams and Follows (2011), DIC can be written as the sum of five components:

$$DIC = \underbrace{DIC^{pi}_{sat} + DIC^{ant}_{sat} + \Delta DIC}_{\text{preformed}} + \underbrace{DIC_{soft} + DIC_{carb}}_{\text{regenerated}} \quad (8)$$

The first three components denote the preformed element (DIC when the water left the surface) while the latter two are the regenerated element (added since subduction).

$DIC^{pi}_{sat}$ and $DIC^{ant}_{sat}$ are the preindustrial and anthropogenic saturated components respectively. They equate to the DIC that the water would have if it were in equilibrium with atmospheric $pCO_2$. They are separated into a preindustrial and anthropogenic part due to the fact that atmospheric $pCO_2$ is not constant, meaning that present day surface waters are equilibrated to higher levels than older waters. In the present analysis, $DIC^{pi}_{sat}$ was calculated using the $CO_2$SYS software in MatLab (van Heuven et al., 2009) with a preindustrial $pCO_2$ of 278 ppm and an estimation for preformed alkalinity (see below). Due to the long equilibration time of the carbonate system, surface waters are rarely saturated in DIC. This is accounted for in the disequilibrium component, $\Delta DIC$. Both $DIC^{ant}_{sat}$ and $\Delta DIC$ are difficult to evaluate directly and are thus collected together in a residual component, $DIC_{res}$ (see Eq. (11)).

The regenerated components, $DIC_{soft}$ and $DIC_{carb}$, are the result of remineralisation of organic matter and dissolution of $CaCO_3$ respectively. The remineralisation of organic matter consumes oxygen and its contribution to DIC is calculated as

$$DIC_{soft} = -r_{CO} * AOU \quad (9)$$

where $r_{CO} = -117/170$ is the stoichiometric ratio of carbon to oxygen (Anderson and Sarmiento, 1994) and $AOU$ (Apparent Oxygen Utilisation) is the difference between the saturated oxygen value, derived from temperature and salinity, and the observed oxygen value (all taken from the CARINA dataset) and so is defined as $AOU = O_{2,sat} - O_{2,obs}$. The dissolution of $CaCO_3$, as well as releasing DIC, also releases alkalinity. Thus it is determined by

$$DIC_{carb} = 0.5 * (Alk_{obs} - Alk_{pre} - r_{NO} * AOU) \quad (10)$$

where $Alk_{obs}$ and $Alk_{pre}$ are the observed (measured) and preformed alkalinity respectively, $r_{NO} = -16/170$ is the stoichiometric ratio of nitrogen to oxygen, $AOU$ is defined as above and the factor of 0.5 accounts for the fact that one unit increase in alkalinity corresponds to a half unit increase in DIC. The $AOU$ term corrects the

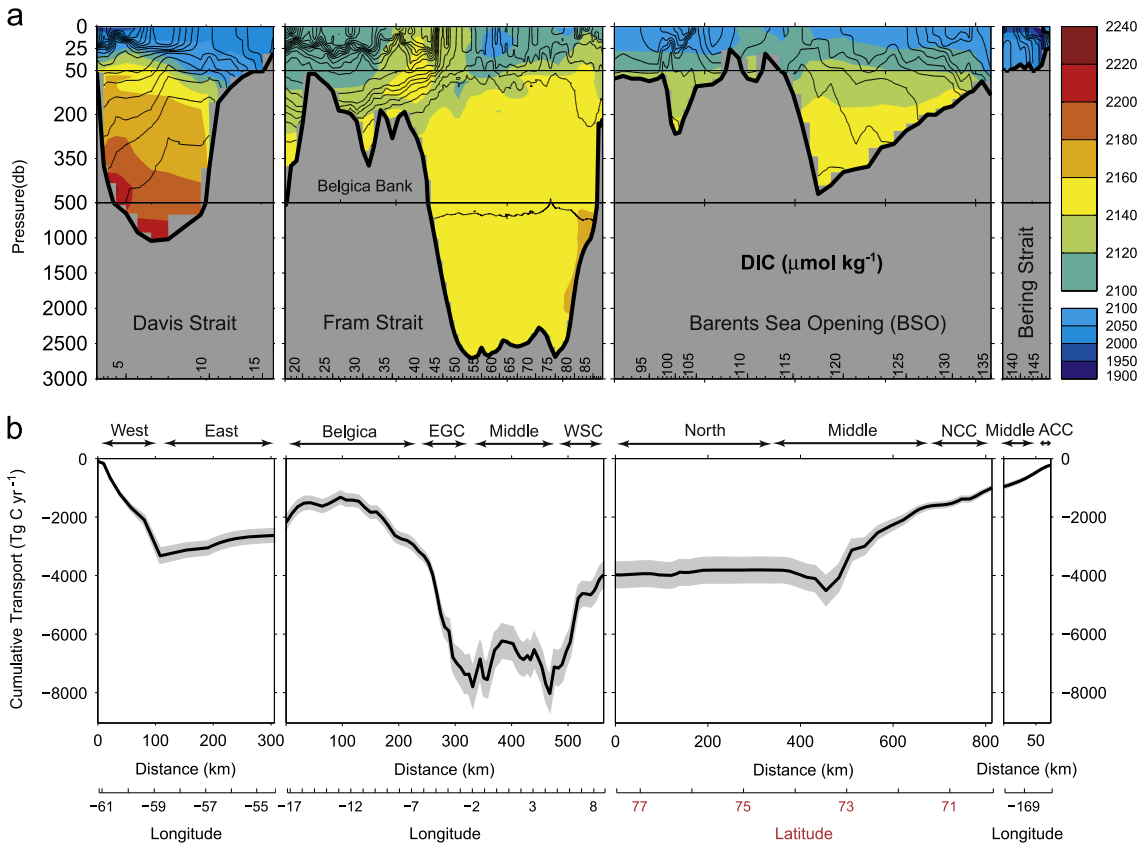


**Fig. 4.** (a) Concentration of DIC across the Arctic Ocean gateways (μmol $kg^{-1}$) taken from the CARINA database and interpolated onto the grid of the hydrographic measurements (see Table 1 for data sources). Black contours denote isopycnals. (b) Cumulative transport of DIC from the west of Davis Strait to the east of Bering Strait. The width of each gateway is scaled according to its actual width and in (a) depths are expanded between 0 and 50 db and between 50 and 500 db.

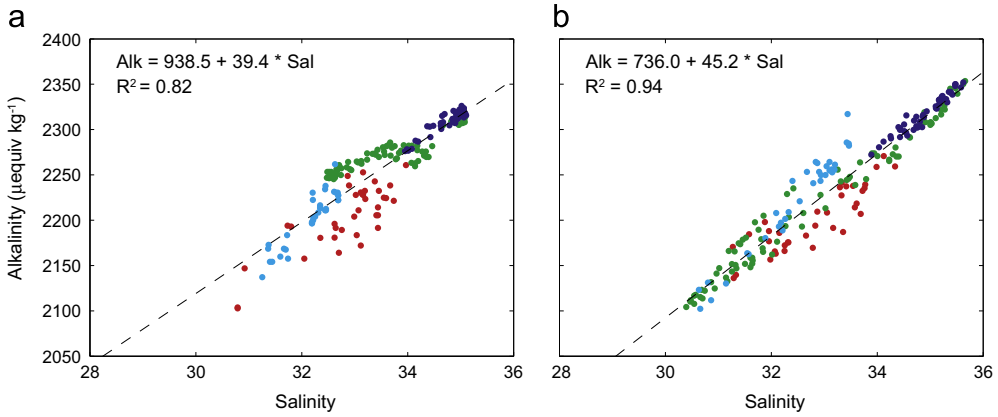


**Fig. 5.** Salinity against alkalinity relationship in the top 100 m for (a) observed data and (b) data after the correction for sea–ice melt and formation. Dashed lines correspond to the line of best fit for the linear regression with the equation given at the top along with the estimate for the correlation ($R^2$). Station 5 in the Bering Strait was omitted from the regression. Data points are coloured by gateway: Davis Strait (red), Fram Strait (green), Barents Sea Opening (dark blue) and Bering Strait (cyan). (For interpretation of the references to colour in this figure caption, the reader is referred to the web version of this paper.)

calculation for the fact that alkalinity is also released, in the form of nitrate, by the remineralisation of organic matter.

Preformed alkalinity ($Alk_{pre}$) was estimated using the close-to-linear relationship between alkalinity and salinity in the surface ocean (Fig. 5). A linear regression was used on measurements in the upper 100 m of the water column across the four gateways. The easternmost station in Bering Strait was omitted from the regression, due to its abnormally high alkalinity and low salinity. While the overall trend is linear (Fig. 5a), with reasonable correlation ($R^2 \approx 0.83$), there is considerable scatter around the regression line and individual gateways, particularly Davis Strait and Fram Strait, exhibit a non-linear relationship due to the effect of sea–ice melt/formation on alkalinity and salinity. Consequently, oxygen isotope data ($\delta^{18}O$; Table 1) were used to determine the fraction of water resulting from sea–ice melt/formation (Yamamoto-Kawai and Tanaka, 2005). Except in Davis Strait, these data were not aligned, spatially or temporally, with the primary bottle data used. However, interpolating the $\delta^{18}O$ data onto the primary bottle locations before calculating the sea–ice fraction reproduced regions of major sea–ice influence that closely corresponded to the regions where the relationship between alkalinity and salinity deviated significantly from the linear trend (i.e. in Davis Strait and over Belgica Bank in Fram Strait). This suggests that the sea–ice effect in these regions is a persistent feature and

that, despite being separated in space and time, the $\delta^{18}O$ data can be used to broadly correct salinity and alkalinity measurements for the influence of sea–ice melt/formation. This was done using end-member concentrations for alkalinity and salinity of 269.3 μmol $L^{-1}$ (Anderson et al., 2004) and 3 (Yamamoto-Kawai and Tanaka, 2005), respectively, and the relationship between corrected measurements showed increased linearity (Fig. 5b). This improvement of the regression strengthens our resolve that the applied correction captures the effect of sea–ice melt/formation on the salinity–alkalinity relationship despite using $\delta^{18}O$ measurements from different datasets. The relationship was subsequently applied to all of the bottle salinity data and the sea–ice correction was reversed to derive $Alk_{pre}$.

Finally, the aforementioned residual component, comprising the anthropogenic and disequilibrium components, was calculated as

$$DIC_{res} = DIC_{sat}^{ant} + \Delta DIC = DIC_{obs} - DIC_{sat}^{pi} - DIC_{soft} - DIC_{carb} \quad (11)$$

where the subscript *obs* denotes total measured DIC. Decomposing DIC into this framework can be used to improve understanding about the processes and mechanisms governing carbon transport in the Arctic Ocean. Net interior (below mixed layer) transport of these components can be equated, with caveats, to terms in the interior transport budget given by Eq. (7). In particular, the combined transport of $DIC_{soft}$ and $DIC_{carb}$ is equivalent to the net transformation term, $T_{int}$. Due to the complications of applying the carbon framework in the mixed layer (Section 3.1), we do not evaluate full depth transports of the components of DIC. For a more detailed explanation of this framework, see chapter 11 of Williams and Follows (2011) or chapter 8 of Sarmiento and Gruber (2006).

### 2.5. Uncertainties

The major uncertainties in our transport calculations are (i) velocity and DIC variability, (ii) the prescription of a fixed mixed layer depth (interior transport only), (iii) measurement asynopticity (full-depth transport only) and (iv) assumptions of the carbon framework (DIC component transports only). We carried out a sensitivity analysis to assess the robustness of our net transport estimates to changes in the velocity field, DIC field and mixed layer depth, thus addressing points (i) and (ii). We addressed asynopticity by considering the effect of variability in mixed layer DIC concentrations (point iii), and dealt with the assumptions of the carbon framework independently (point iv). The derived uncertainties from these analyses are presented in Table 2.

The sensitivity analysis is similar to that adopted by Torres-Valdés et al. (2013). A set of modified velocity fields was prepared in order to represent volume transport uncertainty. A prescribed increase or decrease, corresponding to ±1 standard deviation of mooring velocities over 3 months (T2012), was imposed on the volume transport of the three main Arctic Ocean inflows, through the West Spitsbergen Current, BSO and Bering Strait, and the two main outflows, through Davis Strait and the East Greenland Current. This generated ten different velocity fields in addition to the standard run. Next, a secondary DIC concentration dataset for each gateway (employing measurements from different years) was substituted into DIC transport calculations for each gateway in turn, in order to represent the influence of DIC uncertainty. This approach was not possible for Fram Strait, for which the primary data are the only available full-section measurements, so the impact of DIC uncertainty in this gateway was considered separately (see below). Eleven velocity fields (10 modified, plus the standard) were combined with five DIC concentration fields (the primary and secondary, plus the three available alternates) to give a total of 55 permutations of DIC transport. For interior transport, the prescribed mixed layer depth was also varied in steps of 10 m between 30 and 80 m while using the primary velocity and DIC fields, giving another six calculations. The DIC transport uncertainty is then taken as the standard deviation of all calculations (55 for full-depth transport and 61 for interior transport).

The DIC transport uncertainty for each of the individual inflow or outflow components is larger than the net Arctic DIC transport uncertainty by about an order of magnitude: a few hundred Tg C $yr^{-1}$ compared with a few tens of Tg C $yr^{-1}$ (Table 3). This is a direct consequence of the sensitivity analysis described in the preceding paragraph. Each (independent) permutation of velocity field and DIC concentration field starts from the 'standard solution' velocity field. The increase or decrease to the inflow or outflow volume transport is equivalent to 10–30% of the total. This alteration puts the net pan-Arctic volume transport out of balance, but there is good reason to expect this balance to be closely maintained on timescales longer than a month (see T2012). To allow the components to vary while maintaining net balance, therefore, the inverse model is run again with just two constraints, of total volume and total salinity transport balance. This represents the physical reality that any increase or reduction in component volume transports must (on timescales longer than a month) be balanced by corresponding reductions or increases (respectively) elsewhere. The impact on DIC transports is that a change in one sense in the volume transport of one component will be at least partly offset by the change required by the inversion constraints elsewhere in the opposite sense. The component uncertainties in Table 3 are, therefore, purely local uncertainties. In a pan-Arctic sense, they are not independent and thus do not add in a root-sum-square sense. Indeed, component transport uncertainties within each permutation are strongly anti-correlated. Therefore, net Arctic DIC transport uncertainties are smaller than component uncertainties.

The uncertainty associated with DIC variability in Fram Strait is considered separately to the sensitivity analysis due to a lack of data. Comparison with interannual DIC variability in other gateways, Station M data in the Norwegian Sea (Skjelvan et al., 2008) and interannual nutrient variability in Fram Strait (Torres-Valdés et al., 2013) suggests that DIC in Fram Strait may vary between ±10 and ±100 μmol $kg^{-1}$, and that variability decreases with depth. Consequently, we assume a mean DIC interannual variability across the whole strait of 50 μmol $kg^{-1}$. We multiply this by the volume transport through Fram Strait (full depth −1.6 Sv; interior −1.1 Sv), giving an estimate of DIC transport variability. We use the same concentration variability for $DIC_{soft}$ and $DIC_{res}$ and half the value for $DIC_{sat}^{pi}$ and $DIC_{carb}$ based on the comparative interannual variability of these components in the other gateways.

**Table 2**
Independent uncertainties for net full depth and interior transports for DIC and carbon framework components. All values are in Tg C $yr^{-1}$.

| Uncertainty | Full depth | | | Interior | | |
|---|---|---|---|---|---|---|
| | $DIC$ | $DIC$ | $DIC_{sat}^{pi}$ | $DIC_{soft}$ | $DIC_{carb}$ | $DIC_{res}$ |
| Sensitivity analysis | ±15 | ±10 | ±12 | ±15 | ±8 | ±12 |
| *Fram Strait* | ±31 | ±21 | ±11 | ±21 | ±11 | ±21 |
| Asynopticity | ±35 | NA | NA | NA | NA | NA |
| AOU assumptions | NA | NA | ±3 | ±41 | ±3 | ±47 |
| Total summer uncertainty | ±49 | ±23 | ±17 | ±48 | ±14 | ±53 |
| Total annual uncertainty | ±60 | ±23 | ±17 | ±48 | ±14 | ±53 |

The uncertainty associated with measurement asynopticity results from the variability of DIC concentrations in the surface ocean. We can determine the impact of this by altering the DIC concentration of the upper 50 m of the water column across a range of values representative of summertime DIC variability. By this method, we calculate a plausible range of full-depth summertime transports which we can use to ascribe an uncertainty for asynopticity. This approach is also used to determine the uncertainty associated with adopting our summer transport value as an estimate of annual transport. As for measurement asynopticity, the uncertainty in this assumption is due to surface ocean DIC variability and we can calculate a plausible range of annual transports through altering the upper 50 m DIC concentration across a representative seasonal range.

Since the timing of DIC measurements varies between May and September, the spatial variation of concentrations in the surface ocean of the four main gateways was used to estimate both summertime DIC variability and a representative seasonal range. For the summertime range, we initially calculated the mean DIC concentration in the upper 50 m ($2070 \pm 63$ μmol kg$^{-1}$). Surface concentrations across all four gateways were then set in one case to a constant high value of 2134 μmol kg$^{-1}$ (mean plus standard deviation) and in a second case to a constant low value of 2008 μmol kg$^{-1}$ (mean minus standard deviation). A corresponding range of net DIC transport was then determined and the uncertainty associated with measurement asynopticity was taken as half of this range. To determine a representative seasonal DIC range, we use the fact that despite all of our measurements being taken during summer, some were made later in the productive season than others. An annual low DIC value was calculated as the mean upper 50 m DIC concentration at Davis Strait and Bering Strait (measured towards the end of summer when DIC is depleted after the productive season) *minus* one standard deviation and an annual high value was calculated as the mean upper 50 m concentration at Fram Strait and BSO (measured towards the start of summer before DIC is significantly depleted) *plus* one standard deviation. The resultant range of 1959 to 2135 μmol kg$^{-1}$ is similar to the seasonal range observed in the surface waters of the Norwegian Sea (Skjelvan et al., 2008). Net full-depth transport therefore, with surface concentrations set to these constant high and low values across the four gateways, is assumed to give a plausible estimate of the annual range, with the uncertainty associated with our annual transport estimate taken as half of this range. Due to the weaker seasonal signal beneath the mixed layer, summertime interior transports are assumed to be representative of annual transports without requiring an increase in the uncertainty.

In the transport of the components of DIC, there are further uncertainties associated with the application of the carbon framework. The major uncertainty comes from the possible overestimation of oxygen utilisation (and therefore remineralised DIC) due to the assumptions in calculating AOU, namely that before water leaves the surface, it is fully saturated with respect to oxygen. Modelling studies have shown that this is often not the case at high latitudes, where subducting deep waters are often undersaturated in oxygen (Ito et al., 2004), and an analysis of the CARINA database showed an undersaturation of oxygen in the surface layer of the Nordic Seas (Falck and Olsen, 2010). As a result, AOU can overestimate true oxygen utilisation in waters ventilated in these regions by as much as 20 μmol kg$^{-1}$ (Ito et al., 2004), translating to a possible overestimate of $DIC_{soft}$ by 14 μmol kg$^{-1}$ (using a C:O ratio of 117:170) and of $DIC_{soft}$ and $DIC^{pi}_{sat}$ by $\sim$1μmol kg$^{-1}$ (using a N:O ratio of 16:170). These overestimates then translate to a possible underestimate of $DIC_{res}$ by 16 μmol kg$^{-1}$. To fully evaluate how oxygen undersaturation in sinking waters affects our results would require a detailed understanding of water formation regions and the degree of oxygen undersaturation in those regions, which is beyond the scope of this study. Thus, to deal with the transport uncertainty associated with these potential errors, we consider a worst case scenario in which AOU overestimates oxygen utilisation in major outflows from the Arctic but is accurate in inflows, leading to the maximum possible discrepancy in net transport of the carbon components. We consider specifically the Davis Strait outflow and the East Greenland Current (EGC, western side of deep Fram Strait). The outflows in Davis Strait and the upper waters ($<200$ m) of the EGC partially consist of waters ventilated within the Arctic Ocean (Jahn et al., 2010; Azetsu-Scott et al., 2012), while the deep waters of the EGC were likely to be partially ventilated in the Nordic Seas and modified as they circulated around the Arctic Ocean (Rudels, 1987; Rudels et al., 2005; Marnela et al., 2008). The rapid surface cooling and/or variable ice conditions in these ventilation regions make it plausible that the waters in these outflows were at least partially undersaturated in oxygen when they left the surface, and indeed this has been noted in the Nordic Seas (Falck and Olsen, 2010). To determine the transport uncertainties associated with this, we multiply the combined volume transport of these two outflows beneath 50 m (7.7 Sv; the upper 50 m is not relevant for the transport of the framework components) with the maximum concentration uncertainties given above. The resulting transport uncertainties are presented in Table 2. It should be emphasised that these are conservative estimates of this uncertainty as, in reality, the concentration uncertainty may be lower for many of the water masses. Furthermore, it is likely that inflowing waters would have a similar degree of undersaturation as those in the outflows we identify, since many of them were ventilated in similar regions (e.g. the deep waters of the West Spitsbergen Current or the BSO inflow, both likely to have been partially ventilated in the Nordic Seas), resulting in a lower net effect on the transport of the components than that derived by our calculations.

Further uncertainties associated with the carbon framework include uncertainty in the calculation of preformed alkalinity and the definition of fixed stoichiometric ratios. Variability of preformed alkalinity is induced in the sensitivity runs by the use of alternative datasets for DIC, which alters the salinity–alkalinity relationship that is used. The influence of adopting fixed stoichiometric ratios is small in comparison to the uncertainties associated with the sensitivity runs and the assumptions in calculating *AOU*.

Summertime and annual transport results are presented as the value calculated using the primary velocity field and primary DIC dataset (and a mixed layer depth of 50 m for interior transports) with an uncertainty that is derived by combining the independent uncertainties in a root sum of squares sense (Table 2).

## 3. Results

### 3.1. Carbon framework at the Arctic gateways

Here, we present the results of the carbon framework outlined in Section 2.4. The framework allows us to determine the sources of measured DIC, thereby revealing what processes, such as the remineralisation of organic matter, have led to elevated or depleted concentrations. Figures 6 and 7 show the vertical profiles and cross-sections of the carbon components for each of the four gateways.

In the surface layer, the release of oxygen during primary production leads to negative AOU and consequently to negative $DIC_{soft}$ (Fig. 7b). Furthermore, uncertainty in the estimation of $Alk_{pre}$ results in non-zero values of $DIC_{carb}$ in the surface layer where this component should be negligible, by its definition

(Fig. 7c). These errors feed into $DIC_{res}$, making the carbon framework unreliable in the upper layer of the water column. On the other hand, the approach works well beneath 50 m. Consequently, we evaluate only interior transport values, rather than full-depth values, for the framework components.

In interpreting the carbon framework beneath the mixed layer in each gateway, it is instructive to consider how and why observed DIC differs from the saturated value, $DIC_{sat}^{pi}$, i.e. whether it is elevated by regenerated products or whether the difference is encompassed in the residual component and thus is attributable to disequilibrium or anthropogenic inputs.

The outstanding feature of Davis Strait is the high concentration of $DIC_{soft}$ that increases with depth to values in excess of 100 μmol kg$^{-1}$ (Figs. 6a and 7b). These high values explain almost all of the difference between observed DIC and $DIC_{sat}^{pi}$, with $DIC_{res}$ and $DIC_{carb}$ small by comparison. This suggests that the strong gradient of DIC in Davis Strait is due to the remineralisation of organic matter in subsurface waters. In Fram Strait, observed DIC at intermediate depths (200 to 500 m) is significantly elevated (ANOVA, $p < 0.001$) in comparison to $DIC_{sat}^{pi}$ (Fig. 6b). On the western side of the strait this is due to a contribution from remineralised organic matter (Fig. 7b), while on the eastern side, the difference is encompassed in a high, positive concentration of $DIC_{res}$ (Fig. 7d). The close matching of the latter region with the inflowing West Spitsbergen Current suggests that this signal is contained within northward-flowing Atlantic Water. Beneath 500 m, observed DIC does not increase in the same manner as $DIC_{sat}^{pi}$, despite the addition of up to 40 μmol kg$^{-1}$ of $DIC_{soft}$. Negative $DIC_{res}$, between −10 and −50 μmol kg$^{-1}$, implies that these waters were undersaturated in DIC when they left the mixed layer, with DIC added since then only acting to reconcile observed concentrations with the saturated value. As noted in Section 2.5, $DIC_{res}$ could be underestimated by as much as 16 μmol kg$^{-1}$ in both the deep waters of Fram Strait due to the assumption of 100% oxygen saturation in the calculation of AOU. However, if these waters were undersaturated with respect to oxygen, it is likely that they were also undersaturated with respect to DIC, which has a far longer equilibration time. Indeed, a persistent undersaturation of $fCO_2$ (fugacity of $CO_2$, similar to partial pressure) relative to the atmosphere has been noted in the Greenland Sea throughout winter, when most deep water formation takes place (Anderson et al., 2000). As such, a combination of both processes is likely to be responsible for the negative $DIC_{res}$ in the deep waters of Fram Strait. A similar combination of processes may explain the negative $DIC_{res}$ (between −6 and −25 μmol kg$^{-1}$) in the intermediate and deep waters of Davis Strait.

The prominent feature in BSO is the uniformly high levels of $DIC_{res}$, contributing between 10 and 50 μmol kg$^{-1}$ across much of the region (Fig. 7d). Beneath 50 m, this is almost entirely due to the difference between observed DIC and $DIC_{sat}^{pi}$, with $DIC_{soft}$ and $DIC_{carb}$ making only small contributions. This is particularly true in the southern half of the gateway where, as in Fram Strait, high levels of $DIC_{res}$ are seen in the inflowing Atlantic Water. The high levels of oxygen in shallow Bering Strait, likely due to primary production and/or mixing, mean the application of the framework that produces erroneous results (Fig. 6d).

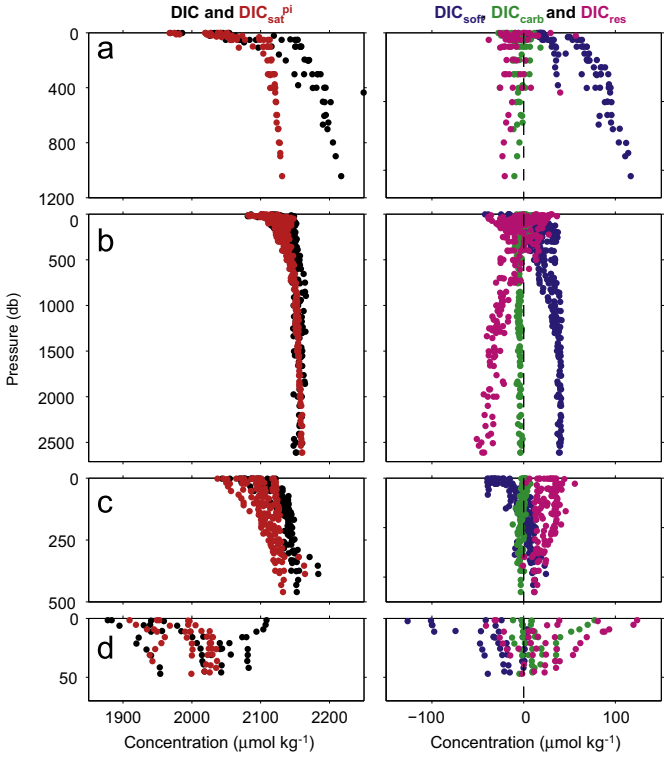


**Fig. 6.** Depth profiles of observed DIC (black) and its components: $DIC_{sat}^{pi}$ (red), $DIC_{soft}$ (blue), $DIC_{carb}$ (green), $DIC_{res}$ (magenta) for (a) Davis Strait, (b) Fram Strait, (c) Barents Sea Opening and (d) Bering Strait in μmol kg$^{-1}$. The height of each profile is scaled relative to the maximum depth of the gateway. (For interpretation of the references to colour in this figure caption, the reader is referred to the web version of this paper.)

### 3.2. DIC transport

We present the transport of DIC across the main Arctic Ocean gateways, evaluated by combining measurements of DIC with the physically consistent velocity field of T2012. This corresponds to the left hand side of Eq. (1) for full depth transport and the left hand side of Eq. (7) for interior transport. In the case of interior transport, we also present the transports of the components of the carbon framework.

#### 3.2.1. Full-depth transport

The cumulative full-depth transport of DIC is shown in Fig. 4, with the values for individual sections presented in Table 3. The Arctic outflow on the west of Davis Strait supports an export of 3320 ± 250 Tg C yr$^{-1}$ (1 Tg = 10$^{12}$ g = 1 Mt), with a small input of 690 ± 80 Tg C yr$^{-1}$ travelling northward in the West Greenland Current, resulting in transport through Davis Strait of −2630 ± 220 Tg C yr$^{-1}$. The main transports in Fram Strait are southward in the East Greenland Current (−4190 ± 730 Tg C yr$^{-1}$) and northward in the West Spitsbergen Current (3150 ± 550 Tg C yr$^{-1}$), leading to net transport of −1350 ± 490 Tg C yr$^{-1}$ across this gateway. Almost all of the DIC imported through BSO, totalling 2980 ± 420 Tg C yr$^{-1}$ is transported in the Atlantic Waters of the middle section (2170 ± 350 Tg C yr$^{-1}$) and in the Norwegian Coastal Current (650 ± 70 Tg C yr$^{-1}$). The Pacific inflow at Bering Strait transports 775 ± 60 Tg C yr$^{-1}$ into the Arctic Ocean.

There is a possible bias in our calculation – towards low import through Bering Strait – caused by extrapolation of DIC concentrations to the western side of this gateway (see Section 2.3). Underestimated DIC of between 100 and 200 μmol kg$^{-1}$ in this section would result in the magnitude of our derived import being underestimated by between 16 and 32 Tg C yr$^{-1}$ (volume transport of 0.41 Sv through this section).

We briefly compare these transports with previous studies that have combined mean DIC concentrations with literature values for volume flows. For a Nordic Seas DIC budget, Jeansson et al. (2011) calculated transport through Fram Strait as −800 ± 1300 Tg C yr$^{-1}$ and through BSO as 1800 ± 300 Tg C yr$^{-1}$. These are considerably lower than transports derived in this paper for the same regions, although the large uncertainty for Fram Strait

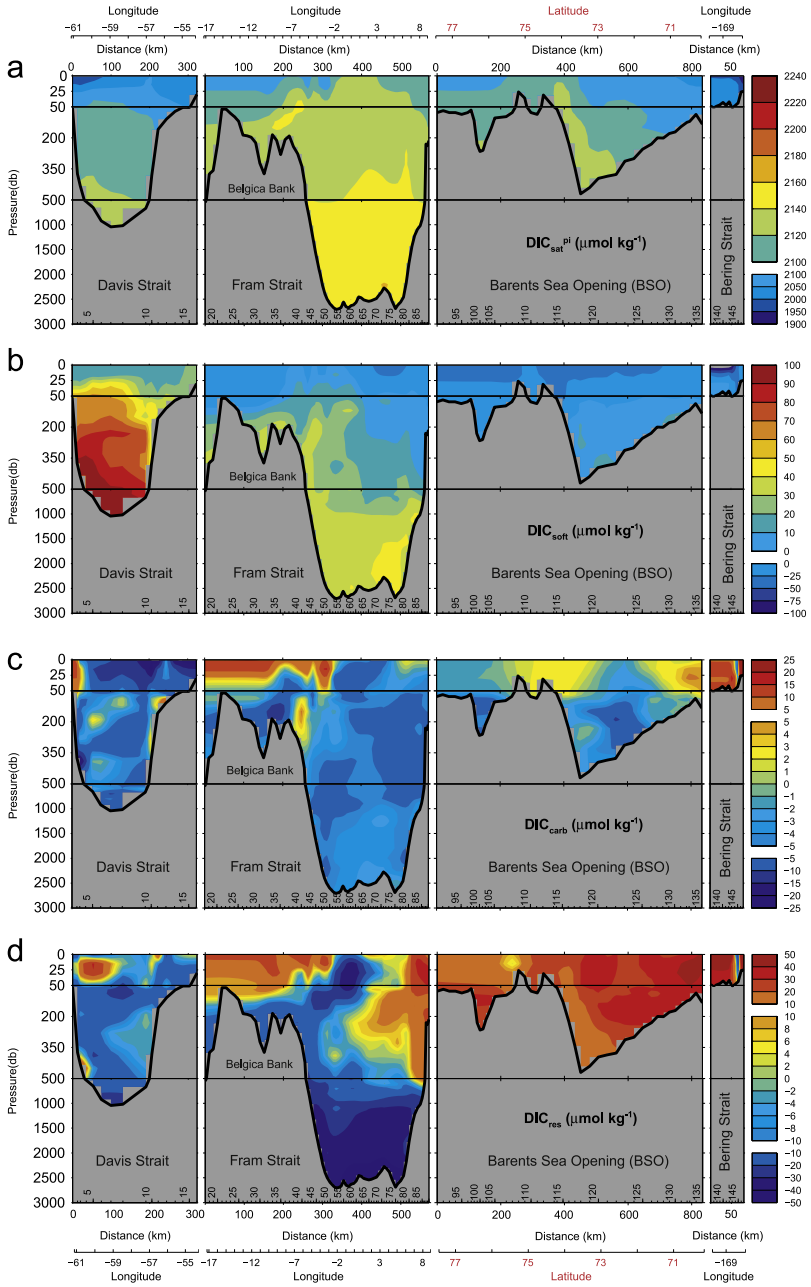


**Fig. 7.** Horizontal section across four gateways for (a) $DIC_{sat}^{pi}$, (b) $DIC_{soft}$, (c) $DIC_{carb}$ and (d) $DIC_{res}$. The width of each gateway is scaled according to its actual width and depths are expanded between 0 and 50 db and between 50 and 500 db. Note that colour scales are different for each component. (For interpretation of the references to colour in this figure caption, the reader is referred to the web version of this paper.)

makes it quantitatively consistent with our estimate. In both cases, the discrepancy is due to the lower volume transports used in the Nordic Seas budget: 1 Sv in comparison to 1.6 Sv for Fram Strait and 2.2 Sv in comparison to 3.6 Sv for BSO. Kivimae et al. (2010) use a volume transport of 3.27 Sv to determine a transport of 2800 Tg C yr$^{-1}$ across BSO, consistent with our estimate. For Davis Strait, no direct estimates of DIC transport were found. Shadwick et al. (2011) calculated the transport of DIC through Jones and Lancaster Sound to the north of Baffin Bay as 1160 Tg C yr$^{-1}$ (updated from the incorrect values printed in the original paper following consultation with the lead author), using a volume transport of 1.4 Sv. This value is quite uncertain, due to the temporal variability of volume transports from the Canadian Arctic Archipelago (CAA; Tang et al., 2004). Nevertheless, we can use it to estimate total DIC transport through the CAA. Assuming that, in 2005, the volume transport through the CAA was equal to the volume transport through Davis Strait (3.1 Sv), and that the DIC properties of waters elsewhere in the CAA are equivalent to those observed in Jones and Lancaster Sound by Shadwick et al. (2011), we estimate total DIC transport through the CAA as *ca.* 2570 Tg C yr$^{-1}$. This is within the uncertainty of the amount of DIC exiting Baffin Bay across Davis Strait (calculated here as $2630 \pm 220$). No comparable DIC transport estimates for Bering Strait were found.

Integrating across all four gateways, net summertime DIC transport from the Arctic Ocean is $-225 \pm 49$ Tg C yr$^{-1}$. Transport of 0.05 Sv of sea–ice across Fram Strait (T2012) exports a further 5.7 Tg C yr$^{-1}$ (sea–ice DIC concentration of 300 μmol kg$^{1}$; Rysgaard et al., 2011) giving an overall export of $231 \pm 49$ Tg C yr$^{-1}$. We adopt this as our primary result, but if we were to account for the possible negative bias mentioned above, this export would be reduced to ca. $207 \pm 50$ Tg C yr$^{-1}$. The large calculated export is in stark contrast

**Table 3**
Volume (Sv) and DIC (Tg C $yr^{-1}$) transports through the four main Arctic Ocean gateways and different sections of each gateway.[a]

| Section | Volume (Sv) | DIC (Tg C $yr^{-1}$) |
|---|---|---|
| **Davis Strait** | $-3.1 \pm 0.3$ | $-2630 \pm 220$ |
| **Fram Strait** | $-1.6 \pm 0.6$ | $-1350 \pm 490$ |
| **BSO** | $3.6 \pm 0.5$ | $2980 \pm 420$ |
| **Bering Strait** | $1.0 \pm 0.1$ | $775 \pm 60$ |
| **Total** | $-0.15 \pm 0.0$ | $-225 \pm 49$ |
| *Davis Strait sections* | | |
| West of 58°W | $-4.0 \pm 0.3$ | $-3320 \pm 250$ |
| East of 58°W | $0.8 \pm 0.1$ | $690 \pm 80$ |
| *Fram Strait sections* | | |
| Belgica Bank (west of 6.5°W) | $-0.7 \pm 0.1$ | $-550 \pm 100$ |
| EGC (6.5°W–2°W) | $-5.0 \pm 0.9$ | $-4190 \pm 730$ |
| Middle (2°W–5°E) | $0.3 \pm 0.6$ | $250 \pm 510$ |
| WSC (east of 5°E) | $3.8 \pm 0.7$ | $3150 \pm 550$ |
| *BSO sections* | | |
| North of 74.5°N | $0.2 \pm 0.0$ | $160 \pm 40$ |
| Middle (71°N–74.5°N) | $2.6 \pm 0.4$ | $2170 \pm 350$ |
| NCC (South of 71°N) | $0.8 \pm 0.1$ | $650 \pm 70$ |
| *Bering Strait sections* | | |
| Middle (west of 168.4°W) | $0.7 \pm 0.1$ | $560 \pm 40$ |
| ACC (east of 168.4°W) | $0.3 \pm 0.0$ | $220 \pm 20$ |

[a] Uncertainty evaluated as standard deviation of 55 runs with varied velocity field and DIC sections. Note that the uncertainties in transport through individual sections are not independent, and thus do not combine to give the net transport uncertainty, which is considerably smaller (see Section 2.5). For total imbalance, uncertainties associated with Fram Strait and measurement non-synopticity are also included (see Table 2).

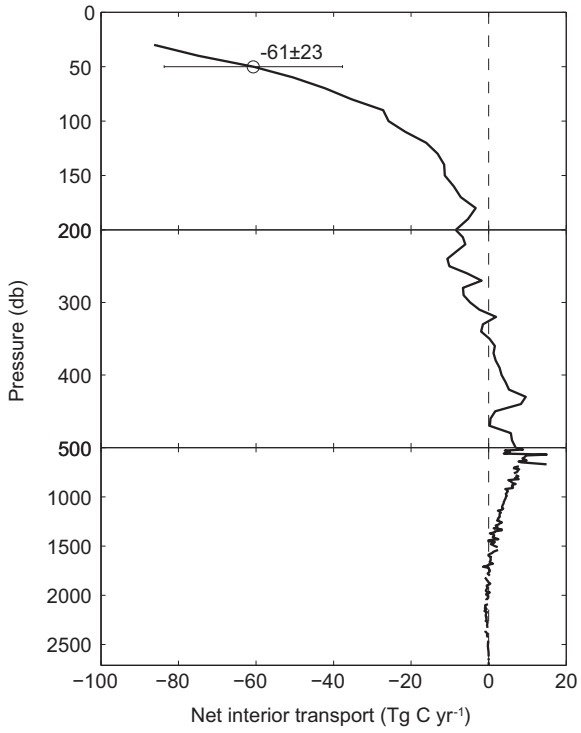


**Fig. 8.** Vertical attenuation of interior transport (in Tg C $yr^{-1}$) for *DIC*. Depths are expanded between 0 and 200 db and between 200 and 500 db. This vertical profile was obtained by increasing the depth of the prescribed interface between the surface and interior ocean in 10 db intervals. The value for a mixed layer depth of 50 m is highlighted.

to the only previous Arctic Ocean carbon budget by Anderson et al. (1998), which calculated a net DIC import of 9 Tg C $yr^{-1}$. Their very different approach was to use a multi-box model with estimated volume transports for the Pacific and Atlantic inflows and between shelf sea boxes and the central basins combined with measured DIC from three cruises in the deep Arctic Ocean, one in the Laptev and Kara Seas and one in the Nordic Seas. Their model does not specifically consider where outflow from the central basins occurs. Rather, the magnitude of the outflows is chosen to balance the inflows and conserve volume, with the outflow DIC concentration for each water mass designated from the central basin cruises. As such, with no DIC measurements in the waters exported across Davis Strait, their carbon budget misses the high DIC concentrations observed in these regions, which our calculations find to be important for net export. Other methodological issues aside, this may contribute to explaining some of the discrepancy between their study and this one.

**Table 4**
Net interior transport of DIC and carbon framework components. Individual terms in the calculation are also shown, net interior transport is the difference between the first and third columns[a]. All values in Tg C $yr^{-1}$ except $\overline{DIC}$ which is in μmol $L^{-1}$.[b]

| Component | $\int\int_{bot}^{mld} v\, DIC\, dxdz$ | $\overline{DIC}$ | $\overline{DIC} \int\int_{bot}^{mld} v\, dxdz$ | **Interior transport** |
|---|---|---|---|---|
| DIC | $-1118 \pm 104$ | $2168 \pm 9$ | $-1057 \pm 101$ | $-61 \pm 23$ |
| $DIC_{sat}^{pi}$ | $-1093 \pm 104$ | $2146 \pm 8$ | $-1046 \pm 99$ | $-46 \pm 17$ |
| $DIC_{soft}$ | $-106 \pm 16$ | $9 \pm 4$ | $-4 \pm 2$ | $-102 \pm 48$ |
| $DIC_{carb}$ | $1 \pm 4$ | $2 \pm 7$ | $-1 \pm 4$ | $2 \pm 14$ |
| $DIC_{res}$ | $78 \pm 13$ | $17 \pm 11$ | $-8 \pm 6$ | $87 \pm 53$ |

[a] For full details of terms and explanation of calculation, see Eq. (7) in Section 2.1.
[b] Uncertainty evaluated as standard deviation of 61 runs with varied velocity field, DIC sections and MLD. For interior transport, uncertainties associated with Fram Strait and assumptions in the carbon framework are also included (see Table 2).

### 3.2.2. Interior transport

Figure 8 shows the change in net interior DIC transport moving from the surface ocean to the ocean interior – evaluated by increasing the depth of the interface for the interior transport calculation from the surface to the deepest measurement. The major export of DIC is achieved in the upper 200 m of the Arctic Ocean, with interior transport attenuating rapidly from the surface to this depth. This implies that most of the full-depth DIC export is achieved in the surface layers, with little net export in the deep ocean. Prescribing a mixed layer depth of 50 m for our primary result, we find net interior transport of DIC of $-61 \pm 23$ Tg C $yr^{-1}$ (Table 4). For the components of the carbon framework, the dominant export is of $DIC_{soft}$ for which the net interior transport is $-102 \pm 48$ Tg C $yr^{-1}$. A transport of $-46 \pm 17$ Tg C $yr^{-1}$ was observed for $DIC_{sat}^{pi}$. The positive net transport of $DIC_{res}$ is $87 \pm 53$ Tg C $yr^{-1}$. The transport of $DIC_{carb}$ of $2 \pm 14$ Tg C $yr^{-1}$ is small by comparison.

The cumulative transports of $DIC_{soft}$, $DIC_{res}$ and $DIC_{carb}$ are shown in Fig. 9. The major transport of $DIC_{soft}$ is achieved through the Arctic outflow in Davis Strait. There is some export through the East Greenland Current in Fram Strait, though this is largely countered by import in the middle section and in the West Spitsbergen Current. Import of $DIC_{res}$ is observed in three regions: western Davis Strait, the East Greenland Current and southern BSO. Referring back to the distribution of $DIC_{res}$ at the gateways (Fig. 7d), import in the southward moving waters of Davis Strait and the East Greenland Current is due to the export of negative $DIC_{res}$, while import in the southern half of BSO is the result of high positive $DIC_{res}$ in the inflowing Atlantic Water. There is a similar

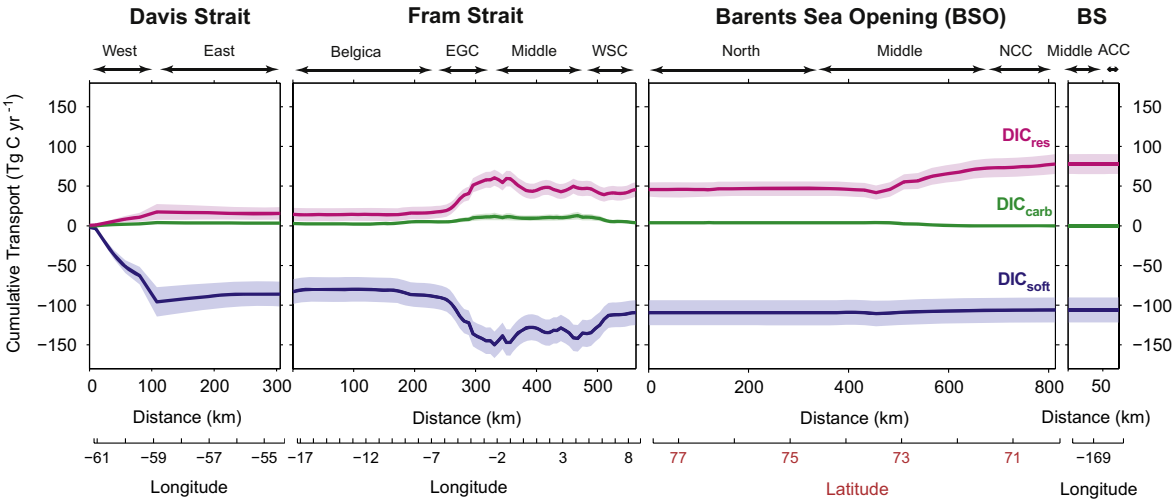


**Fig. 9.** Cumulative interior transport of $DIC_{soft}$, $DIC_{carb}$ and magenta $DIC_{res}$. Note that these sectional values are uncorrected and do not represent transport under volume conservation, hence the final imbalance here is not exactly equal to corrected net interior transport. (For interpretation of the references to colour in this figure caption, the reader is referred to the web version of this paper.)

positive contribution from the high $DIC_{res}$ in the inflowing intermediate waters of the West Spitsbergen Current, but it is not visible in the net transports of Fig. 9 due to negative $DIC_{res}$ in the deep waters beneath. There is little discernable pattern in $DIC_{carb}$ transport.

## 4. Discussion

Using Eqs. (1) and (7) for full-depth and interior transport respectively, we consider the net DIC transports presented in Section 3.2 in the context of the pan-Arctic DIC budget. We use published values as well as the carbon framework to estimate the terms on the right hand side of these equations, closing the budget and allowing us to calculate uncertain values such as the air–sea flux of $CO_2$ and the sequestration of carbon across 50 m.

### 4.1. Full-depth transport and the air–sea $CO_2$ flux

By our calculation, there is net full-depth summertime DIC export from the Arctic Ocean of $231 \pm 49$ Tg C yr$^{-1}$. This value could be biased high due to the underestimation of transport through western Bering Strait (Section 3.2.1), potentially reducing export to $207 \pm 50$ Tg C yr$^{-1}$. For the purpose of comparison with other terms in the carbon budget, we take our primary result ($231 \pm 49$ Tg C yr$^{-1}$) to be representative of annual transport, with increased uncertainty of $\pm 60$ Tg C yr$^{-1}$ (see Section 2.5 for uncertainty calculation). This export must be the result of surface fluxes, net transformation of DIC and/or changes in DIC storage within the Arctic Ocean (Eq. 1). Here, we use published values to estimate the magnitude of most of these terms, leaving a residual that we interpret as the air–sea $CO_2$ flux. A schematic representation of the terms in the Arctic Ocean DIC budget is shown in Fig. 10 and the origin of these terms is discussed below.

The surface DIC flux, $F_s^{DIC}$, comprises freshwater inputs ($F_{FW}^{DIC}$) and air–sea gas exchange ($F_{AS}^{DIC}$). In the inverse model velocity field freshwater inputs result in a volume divergence of 0.19 Sv (T2012) which is the net result of river inputs, precipitation and evaporation. We assume that the transport of DIC in precipitation and evaporation is negligible. A comprehensive sampling programme of the main Arctic rivers has led to a recent estimate for the annual pan-Arctic riverine DIC flux of $57 \pm 9.9$ Tg C yr$^{-1}$ (Tank et al., 2012). Removing fluxes into the Bering Sea, Hudson Bay and Hudson Strait, which are not part of our Arctic Ocean box, reduces

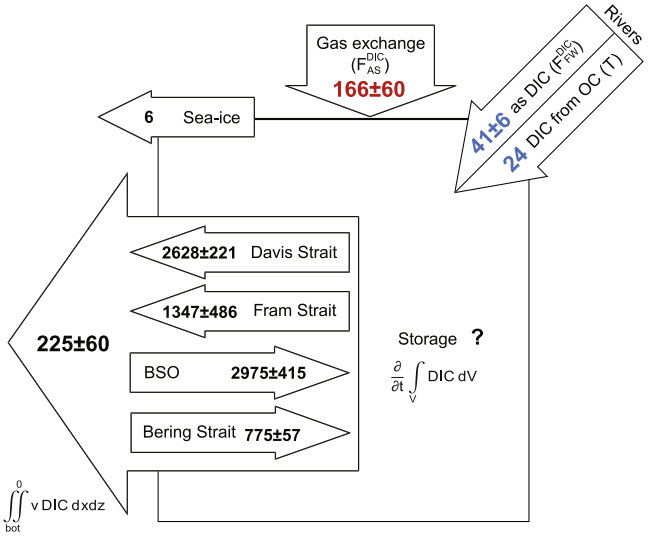


**Fig. 10.** Summary figure of the terms in the full-depth Arctic Ocean DIC budget (Eq. (1)). Terms calculated in this study are in black, those taken from the literature are in blue and the residual of the DIC budget (the air–sea exchange estimate) is in red. All values are in Tg C yr$^{-1}$. *Note*: the uncertainties in transport through individual gateways are not independent, and thus do not combine to give the net transport uncertainty, which is considerably smaller (see Section 2.5). (For interpretation of the references to colour in this figure caption, the reader is referred to the web version of this paper.)

this value to $40.8 \pm 6.4$ Tg C yr$^{-1}$. Accounting for this input leaves a residual export of $190 \pm 60$ Tg C yr$^{-1}$. Before asserting this residual to be an estimate of the air–sea $CO_2$ flux, we proceed to examine net transformation of DIC within the Arctic Ocean.

Net transformation within the ocean boundaries, $T$, can be separated into changes between DIC and particulate inorganic carbon ($T^{PIC}$), the result of net dissolution or formation of $CaCO_3$, and between DIC and organic carbon ($T^{OC}$), determined by the balance of the Arctic Ocean organic carbon budget. We first assume that there is a negligible contribution from $T^{PIC}$, i.e. that any $CaCO_3$ formed in primary production is dissolved in the water column. This assumption is supported by the minimal net interior transport observed for $DIC_{carb}$, which suggests net balance of $CaCO_3$ across the Arctic Ocean. With respect to $T^{OC}$, we assume that the marine-derived component of the organic matter budget is in approximate balance. This is supported by the budget

calculation of MacDonald et al. (2010) who suggested that less than 3% of marine organic carbon is buried, with the rest being remineralised in the region. High inputs of terrigenous organic carbon to the Arctic Ocean, however, may result in positive $T^{OC}$ as this carbon remineralises. Raymond et al. (2007) calculated an annual riverine dissolved organic carbon flux to the Arctic Ocean of 25 Tg C $yr^{-1}$. More recently, Holmes et al. (2012) evaluated an equivalent flux of 30 Tg C $yr^{-1}$ (reduced here from the original 34 Tg C $yr^{-1}$ for the whole Arctic watershed). This, in combination with estimates of particulate organic carbon inputs from rivers ($5 \pm 1$ Tg C $yr^{1}$; Dittmar and Kattner, 2003) and coastal erosion (6.7 Tg C $yr^{1}$; Rachold et al., 2004) suggests an annual terrigenous organic carbon influx of 42 Tg C $yr^{-1}$. A large proportion of this input was traditionally thought to be recalcitrant (Dittmar and Kattner, 2003; Amon, 2004), remaining in its organic form until sedimentation or export from the Arctic Ocean. Recent work, however, suggests that asmuch as 80% of the dissolved fraction is remineralised to DIC (Hansell et al., 2004; Alling et al., 2010; Letscher et al., 2011). Adopting this upper limit, and assuming that the remineralisation of particulate organic carbon is negligible, we derive a conservative estimate for $T^{OC}$ (and therefore $T$) of 24 Tg C $yr^{-1}$, leaving a residual export of $166 \pm 60$ Tg C $yr^{-1}$. This constitutes an 11% reduction as a result of the remineralisation of riverine dissolved organic matter.

Returning to the DIC budget, equating the residual export to an estimate of the air–sea flux, $F_{AS}^{DIC}$, depends on the possible change in storage of DIC in the Arctic Ocean ($\partial/\partial t \int_{intV} DIC\, dV$). As a result of constantly rising atmospheric $pCO_2$, it is likely that the region is accumulating DIC, making this term positive. Indeed, this was noted in the budget calculations of Anderson et al. (1998) and here it is qualitatively shown at least to be occurring beneath the surface ocean (Section 4.2). Thus, we propose a lower bound for annual air–sea $CO_2$ uptake by the Arctic Ocean of $166 \pm 60$ Tg C $yr^{-1}$. Even as a lower bound, this is at the upper end of the conventional range of 66–199 Tg C $yr^{-1}$ derived from a synthesis of pan-Arctic studies and extrapolated regional estimates (Bates and Mathis, 2009). It is considerably greater than direct pan-Arctic estimates derived from a previous carbon budget ($24 \pm 17$ Tg C $yr^{1}$; Anderson et al., 1998), biogeochemical models (59 Tg C $yr^{1}$, $58 \pm 6$ Tg C $yr^{1}$; Manizza et al., 2011, 2013) and satellite estimations ($118 \pm 7$ Tg C $yr^{1}$; Arrigo et al., 2010). There are important inconsistencies in the area definition of the Arctic Ocean between all of these studies. As previously noted, the carbon budget of Anderson et al. (1998) did not resolve outflow through Davis Strait (Section 3.2.1) while Bates and Mathis (2009) did not include direct estimates of uptake in the Canadian Arctic Archipelago or Baffin Bay due to limited data. Given the importance of these regions to our calculation (Section 4.2), this omission may partially explain why their estimates differ from ours. On the other hand, the domains of Arrigo et al. (2010) and Manizza et al. (2011, 2013) include Baffin Bay and even the Greenland Sea (not included in our study) making it likely that their lower values are the result of methodological differences.

Our derived air–sea $CO_2$ flux suggests that the Arctic Ocean is responsible for ~10 to 12% of present day global oceanic carbon uptake: $1400 \pm 700$ Tg C $yr^{-1}$ ($pCO_2$ climatology; Takahashi et al., 2009) and $1700 \pm 400$ Tg C $yr^{-1}$ (global inversion; Gruber et al., 2009). With a surface area that constitutes only 3% of the global ocean, this supports the hypothesis that the Arctic Ocean plays a disproportionately important role in global oceanic carbon uptake (Bates and Mathis, 2009).

### 4.2. Interior transport and the Arctic Ocean carbon pumps

For our primary interior transport results we adopted a mixed layer depth of 50 m, beneath which the net DIC transport is $-61 \pm 23$ Tg C $yr^{-1}$. According to the interior ocean DIC budget (Eq. (7)) this is the result of three processes: net transformation of organic (and particulate inorganic) carbon to DIC beneath the mixed layer; net downwelling of high DIC waters across the mixed layer base; and the change in DIC storage of the interior ocean. We use the carbon framework to infer the relative contribution of these processes to the total export. A summary of the transports of the carbon framework components is presented in Fig. 11.

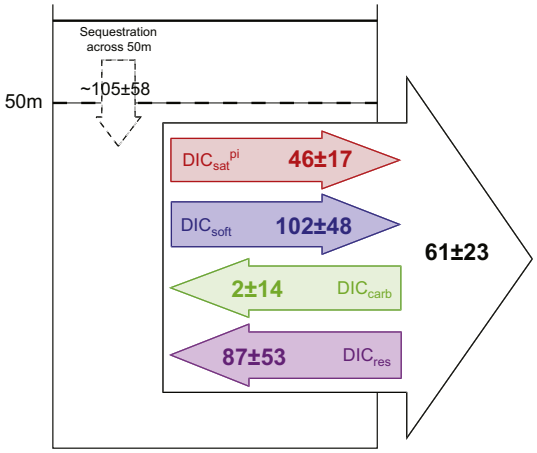


**Fig. 11.** Summary figure of the interior transport of DIC and the components of the carbon framework, as well as an estimate of volume-conserved sequestration across the 50 m mixed layer depth. All values are in Tg C $yr^{-1}$.

Net transport of DIC originating from the remineralisation of organic matter, $DIC_{soft}$, is equivalent (though opposite in sign) to the net transformation term, $T_{int}$, in Eq. (7) (considering that the contribution from the dissolution of particulate inorganic carbon, $DIC_{carb}$, is negligible). As such, $DIC_{soft}$ export of $102 \pm 48$ Tg C $yr^{-1}$ (almost twice as great as the observed DIC export) indicates the importance of $T_{int}$ in the Arctic Ocean interior DIC budget. As noted in Section 2.1, $T_{int}$ may be interpreted as a measure of the strength of the biological pump. This is because it equates to the amount of DIC added to the ocean interior from the sinking and subsequent remineralisation of organic matter across the mixed layer base. One caveat to this interpretation is the possible additional remineralisation of organic carbon that has originated from external sources, such as terrigenous inputs, which we have previously noted as significant (Section 4.1). However, it is likely that the majority of this remineralisation occurs in the coastal zone (Alling et al., 2010; Holmes et al., 2012) and surface ocean (Letscher et al., 2011). As such, we assume that remineralisation of terrigenous organic carbon is negligible in the ocean interior and that $T_{int}$ is equivalent to the marine biological pump. A value of $102 \pm 26$ Tg C $yr^{-1}$, therefore, suggests that the biological pump is a significant source of DIC to the Arctic Ocean interior. A recent estimate of primary production in the Arctic Ocean derived from satellites suggested an average of $335.7 \pm 33.5$ Tg C $yr^{-1}$ between 1998 and 2009 (Brown and Arrigo, 2012; contribution from Greenland Sea section removed) while the budget calculation of MacDonald et al. (2010) derived a value of 361 Tg C $yr^{-1}$. The calculation of this study, therefore, suggests that up to 30% of this organic matter is transported beneath 50 m before being remineralised and exported across the Arctic Ocean boundaries.

The importance of the biological pump is further emphasised by the vertical profile of interior transport (Fig. 8). The absolute majority of DIC export is shallower than 200 m, which is marginally deeper than the approximate mean depth of the extensive Arctic Ocean shelf seas (Carmack and Wassmann, 2006). This hints at the importance of shelf sea processes such as the continental shelf pump in exporting DIC beneath the mixed layer and into the Arctic Ocean halocline (Anderson et al., 2010, 2013).

In addition to shelf sea processes contributing to shallow water export, elevated DIC in the intermediate and deep outflowing waters of Davis Strait makes an important contribution to net export from the Arctic Ocean. The carbon framework suggests that high concentrations at Davis Strait are also the result of the biological pump (high $DIC_{soft}$, Fig. 7b). The origin of this $DIC_{soft}$, and the organic matter from which it is derived, is therefore central to understanding the role of the biological pump in exporting DIC from the Arctic Ocean. This Arctic outflow may have high levels of $DIC_{soft}$ due to its origin in the DIC enriched halocline of the central Canadian Basin (Azetsu-Scott et al., 2010), linking it to the shelf sea processes mentioned above, or by the addition and remineralisation of organic matter during flow through the CAA (Shadwick et al., 2011) or Baffin Bay. Nutrient studies suggest that biological processes in North Water polynya (at the northern end of Baffin Bay) are responsible for elevated concentrations of nitrate, phosphate and silicate in the deep water masses of Baffin Bay (Tremblay et al., 2002; Michel et al., 2002; Torres-Valdés et al., 2013). They attribute this to the high production of diatoms in this region, whose silica shells resist dissolution and transport organic matter beneath the mixed layer before it is remineralised. Indeed, vertical export of organic matter out of the mixed layer at North Water polynya has been noted to be greater than other regions in the Arctic Ocean (Lalande et al., 2009a) and as high as 60% of primary production (Garneau et al., 2007). The importance of elevated $DIC_{soft}$ at Davis Strait for the export of DIC from the Arctic Ocean and the potentially important contribution from biological activity in the North Water polynya to these elevated concentrations, suggests that the biological pump in this region might play a central role in removing carbon from the surface to the deep ocean in the Arctic.

We now consider the vertical eddy transport term of Eq. (7), $\int w'DIC'\,dA$. A negative value (since $w'$ is positive upward) implies that, within the Arctic Ocean boundaries, downward-moving waters have higher DIC concentration than those moving upward. The potential for this to be the case in the Arctic Ocean is suggested by the export of $46 \pm 17$ Tg C yr$^{-1}$ of $DIC^{pi}_{sat}$. The distribution of this component is largely controlled by changes in temperature and salinity, which affect the solubility of $CO_2$ in seawater. The fact that, within the ocean boundaries, there is a source of $DIC^{pi}_{sat}$, implies that there is a net input of low-temperature and/or high-salinity water across the mixed layer, with the potential to hold high concentrations of DIC. This is consistent with the Arctic's role in dense water formation, either through the cooling and subduction of Atlantic Water or the sinking of cold, saline, DIC-enriched waters resulting from brine rejection. These processes have been hypothesised to play an important role in Arctic Ocean carbon sequestration (Anderson et al., 1999; Fransson et al., 2001; Kaltin et al., 2002; Anderson et al., 2004; Rysgaard et al., 2011). The export of $DIC^{pi}_{sat}$ suggests that sinking waters have the capacity to be DIC-enriched but, due to possible disequilibria or anthropogenic inputs, does not quantify their actual contribution to physical DIC transport. Thus this quantity is not directly equivalent to the vertical eddy transport term in Eq. (7).

For the purpose of considering processes within the Arctic Ocean boundaries, volume conservation is preserved in net interior transport calculations. However, volume imbalance across certain depth ranges may indicate a more significant role of the Arctic Ocean in moving DIC beneath the mixed layer by physical processes. Convergence of volume in the upper 50 m (Section 2.2) and subsequent sinking beneath the mixed layer transports a large amount of DIC to the ocean interior – a contribution that we remove when calculating interior transport (second term on left hand side of Eq. (7)). Depending on the DIC concentration of this water when it returns to the surface layer outside the Arctic Ocean, this vertical movement of DIC may contribute to carbon sequestration on a global scale. Quantifying this contribution is beyond the scope of this study, hence we consider volume-conserved processes only.

The final element to be considered is the potential change in storage of DIC within the ocean boundaries. This can be partly understood through analysing the residual component of the carbon framework, $DIC_{res}$. The combined exports of $DIC_{soft}$ ($102 \pm 48$ Tg C yr$^{-1}$) and $DIC^{pi}_{sat}$ ($46 \pm 17$ Tg C yr$^{-1}$) imply that the amount of DIC exported should be greater than that which is observed ($61 \pm 23$ Tg C yr$^{-1}$) – a discrepancy that is accounted for in the import of $87 \pm 53$ Tg C yr$^{-1}$ of $DIC_{res}$. This import is achieved in approximately equal measure through the export of negative $DIC_{res}$ (in the intermediate and deep waters of Davis Strait and Fram Strait) and the import of positive $DIC_{res}$ (in the Atlantic Waters of Fram Strait and BSO) as noted in Section 3.2.2. Assuming that calculation of all other components in the carbon framework is accurate, $DIC_{res}$ is made up of anthropogenic carbon ($DIC^{ant}_{sat}$) and a disequilibrium ($\Delta DIC$). The anthropogenic contribution is always positive, so that negative values of $DIC_{res}$ must be the result of a negative disequilibrium (i.e. undersaturation on subduction). Thus, export of negative $DIC_{res}$ (as in Davis Strait and western Fram Strait) implies that, in reality, less DIC is exported than has been inferred from the saturated component, $DIC^{pi}_{sat}$. On the other hand, positive $DIC_{res}$ could result from both an anthropogenic source and/or a positive disequilibrium (i.e. supersaturation on it subduction). Recent literature supports the hypothesis that the positive $DIC_{res}$ observed in Atlantic Waters is primarily due to anthropogenic $CO_2$. Olsen et al. (2010) and Tanhua et al. (2009) used measurements of CFCs to determine the inventory of anthropogenic carbon in the Nordic Seas and central Arctic Ocean respectively. Both studies identify higher $DIC^{ant}_{sat}$ in waters of Atlantic origin, attributing this signal to the higher uptake capacity (lower Revelle factor) of the warm, saline Atlantic Water. Jeansson et al. (2011) also used CFCs to determine the high concentrations of $DIC^{ant}_{sat}$ in Atlantic Waters crossing the Nordic Sea boundaries. Rather than $CO_2$ being taken up in transit through the Nordic Seas, these waters are already rich in $DIC^{ant}_{sat}$ when they enter from the North Atlantic, suggesting that uptake in the lower latitudes is responsible. Both global observational studies (Sabine et al., 2004; Khatiwala et al., 2009) and simple advective models (Anderson and Olsen, 2002) support this suggestion, identifying the North Atlantic as an important region for the uptake of anthropogenic carbon.

The measured import of $DIC_{res}$, therefore, indicates that the Arctic Ocean interior is accumulating anthropogenic carbon through high concentrations in Atlantic Water. This may have significant consequences for the Arctic Ocean carbon system, with the potential to ultimately change from a net exporter to a net importer of DIC. Outward transport of $DIC^{ant}_{sat}$ will increase as Atlantic Water circulates and leaves the Arctic and as more is taken up from the atmosphere within the ocean boundaries. However, with water in the North Atlantic taking up increasing amounts of anthropogenic $CO_2$ as atmospheric concentrations rise, the anthropogenic component of inflowing waters is likely to remain higher than those leaving, meaning that accumulation will continue into the foreseeable future. Acting as a partial terminus for northward moving anthropogenic $CO_2$, therefore, the Arctic Ocean's current role as a net exporter of DIC may be diminished or reversed in the future.

At the same time as anthropogenic carbon accumulates in the Arctic Ocean, changes to the biological and physical pumps in a warming climate may also impact interior DIC transport, with associated changes in the transport of the carbon framework components. Observations suggest a strengthening of the biological pump as sea–ice diminishes (Pabi et al., 2008; Arrigo et al., 2008; Lalande et al., 2009a), an effect that would be marked by an increase in the export of $DIC_{soft}$. Increased input and remineralisation of terrigenous organic matter (McGuire et al., 2009) would also increase the export of $DIC_{soft}$, meaning that changes in the

transport of this component would not necessarily imply a change in the biological pump alone. Export of $DIC_{sat}^{pi}$ may decrease as Arctic waters warm and freshen, but further impacts such as increased upwelling and decreased sea–ice cover will influence $\Delta DIC$ (and consequently $DIC_{res}$) in uncertain ways such that changes in the physical pump will be difficult to quantify.

Finally, we estimate the volume-conserved biological and physical sequestration of DIC across 50 m within the Arctic Ocean. This sequestration estimate is denoted 'volume-conserved' to highlight the fact that it does not quantify the possible contribution to sequestration from the net sinking of water across 50 m in the Arctic Ocean (see above). We adjust net interior DIC transport for an estimated accumulation of anthropogenic carbon and assume that, aside from this accumulation, the carbon budget is in steady state, i.e. we resolve the storage term in Eq. (7), leaving a residual that we equate to carbon sequestration. We assume that the net transport of $DIC_{res}$ is due in equal parts to the import of $DIC_{sat}^{ant}$ and the export of negative $\Delta DIC$. This suggests an accumulation of $44 \pm 53$ Tg C yr$^{-1}$ of anthropogenic carbon in the ocean interior, which is in reasonable agreement with Jeansson et al. (2011) who found that $58 \pm 15$ Tg C yr$^{-1}$ of anthropogenic carbon is imported in Atlantic Water across the full-depth range. Removing this anthropogenic input from net interior DIC transport gives a value of $105 \pm 58$ Tg C yr$^{-1}$ for volume-conserved sequestration across 50 m (Fig. 11). Comparing this to the estimated uptake of $CO_2$ from the atmosphere ($166 \pm 60$ Tg C yr$^{-1}$), around 60% appears to be sequestered beneath 50 m. The similarity of this estimate to our calculation of the biological pump ($102 \pm 48$ Tg C yr$^{-1}$) suggests that this mechanism is the dominant control on Arctic Ocean carbon sequestration across 50 m, and that volume-conserved physical sequestration is of little importance. Observations of $pCO_2$ in the Canadian Basin suggest that decreasing sea–ice cover will not significantly strengthen the Arctic Ocean carbon sink (Cai et al., 2010; Else et al., 2013b). Our calculations, on the other hand, suggest that a strengthening of the biological pump (Arrigo et al., 2008; Lalande et al., 2009a; Brown and Arrigo, 2012) could drive an increase in Arctic Ocean carbon uptake, consistent with the model results of Manizza et al. (2013).

## 5. Conclusions

Through an observation based approach, this study has established baseline estimates for the transport of DIC across the main Arctic Ocean gateways. As such, it provides a means of validating an increasing number of models being used to examine the region's carbon cycle (e.g. Manizza et al., 2011, 2013) and offers a reference against which to evaluate future changes. We also calculated the relative contributions of physical and biological processes to DIC concentrations and transports, through the application of a carbon framework (Williams and Follows, 2011).

We have shown that the Arctic Ocean is exporting $225 \pm 49$ Tg C yr$^{-1}$ of DIC across the full depth range, with a further 5.7 Tg C yr$^{-1}$ exported in sea–ice. Budget considerations suggest that on an annual basis, at least $166 \pm 60$ Tg C yr$^{-1}$ of this export is due to uptake of $CO_2$ from the atmosphere. Even as a lower bound, this is greater than previous pan-Arctic estimates, although where the Arctic Ocean boundaries are defined is important. In particular, this work has highlighted the important role of Davis Strait and Baffin Bay, emphasising the need for ongoing monitoring of this region. This study underlines the global importance of the Arctic Ocean as a $CO_2$ sink.

We calculate DIC export from the ocean interior (beneath 50 m) as $61 \pm 23$ Tg C yr$^{-1}$, suggesting that most of the full-depth export is achieved in the surface layer. The utility of the carbon framework is portrayed in identifying the important role of the biological pump in the Arctic Ocean, with the suggestion that up to 30% of the region's marine-derived organic matter is transported vertically across 50 m. Furthermore, the framework qualitatively highlights the accumulation of anthropogenic $CO_2$ in the Arctic Ocean. Accounting for this, we suggest a volume-conserved carbon sequestration across 50 m of $105 \pm 58$ Tg C yr$^{-1}$.

## Acknowledgements

This paper is a contribution to the TEA-COSI project of the UK NERC's Arctic Research Programme (Grant no. NE/I028947/1). The work was conducted as part of an MSc for Ocean and Earth Science, University of Southampton. Dissolved inorganic carbon data were taken from the CARINA Data Synthesis Project (http://cdiac.ornl.gov/oceans/CARINA/) except in Davis Strait. We are grateful to the carbon PI's from various expeditions for making these data available: Peter Jones (Davis Strait, 1997); Richard Bellerby (eastern Fram Strait and BSO, 2002); Leif Anderson (western Fram Strait, 2002); Truls Johannessen and Are Olsen (BSO, 2003); Nick Bates (Bering Strait, 2002); Louis Codispoti and James Swift (Bering Strait, 2004). For Davis Strait, we are grateful to Craig Lee and Brian Petrie for cruise organisation and physical data/sampling, and to Richard Fairbanks and Rick Mortlock for $\delta^{18}O$ data. Davis Strait data collection was funded by the U.S. National Science Foundation Freshwater Initiative (2004–2007), the International Polar Year (IPY) and Arctic Observing Network (2007–2010) programs under Grant nos. OPP0230381 and OPP0632231. Additional support was provided by the N-CAARE, Department of Fisheries and Oceans, Canada, and IPY-Canada. We are also grateful to Lee Cooper for making $\delta^{18}O$ data available for Bering Strait (collected as part of the RUSALCA project; http://www.arctic.noaa.gov/aro/russian-american/) and Andreas Mackensen for $\delta^{18}O$ data in Fram Strait. In BSO, $\delta^{18}O$ data were taken from the Global Seawater Oxygen-18 Database – v1.21 (http://data.giss.nasa.gov/o18data/). We would like to thank Ric Williams and John Lauderdale for guidance on the carbon framework and Nick Bates for comments on DIC in the western side of Bering Strait. Finally, we are grateful to two anonymous reviewers for their comments on an original draft of this paper.

## References

Alling, V., Sanchez-Garcia, L., Porcelli, D., Pugach, S., Vonk, J.E., van Dongen, B., Mörth, C.M., Anderson, L.G., Sokolov, A., Andersson, P., Humborg, C., Semiletov, I., Gustafsson, O., 2010. Nonconservative behavior of dissolved organic carbon across the Laptev and East Siberian Seas. Global Biogeochem. Cycles 24, GB4033, http://dx.doi.org/10.1029/2010GB003834.

Amon, R.M.W., 2004. The role of dissolved organic matter for the organic carbon cycle in the Arctic Ocean. In: Stein, R., Macdonald, R.W. (Eds.), The Organic Carbon Cycle in the Arctic Ocean. Springer, Berlin, pp. 33–55

Anderson, L., 2007. Oden 77DN20020420 cruise data from the 2002 cruises, CARINA data set. Technical report, Carbon Dioxide Information Analysis Center, Oak Ridge National Laboratory, Department of Energy, Oak Ridge, Tennessee, US, http://dx.doi.org/10.3334/CDIAC/otg.CARINA_77DN20020420.

Anderson, L.A., Sarmiento, J.L., 1994. Redfield ratios of remineralization determined by nutrient data-analysis. Glob. Biogeochem. Cycles 8 (1), 65–80, http://dx.doi.org/10.1029/93GB03318.

Anderson, L.G., Olsen, A., 2002. Air–sea flux of anthropogenic carbon dioxide in the North Atlantic. Geophys. Res. Lett. 29 (17), 1835, http://dx.doi.org/10.1029/2002GL014820.

Anderson, L.G., Olsson, K., Chierici, M., 1998. A carbon budget for the Arctic Ocean. Glob. Biogeochem. Cycles 12 (3), 455–465, http://dx.doi.org/10.1029/98GB01372.

Anderson, L.G., Jones, E.P., Rudels, B., 1999. Ventilation of the Arctic Ocean estimated by a plume entrainment model constrained by CFCs. J. Geophys. Res. 104 (C6), 13423–13429, http://dx.doi.org/10.1029/1999JC900074.

Anderson, L.G., Drange, H., Chierici, M., Fransson, A., johannessen, T., Skjelvan, I., Rey, F., 2000. Annual carbon fluxes in the upper Greenland Sea based on measurements and a box-model approach. Tellus B 52 (3), 1013–1024, http://dx.doi.org/10.1034/j.1600-0889.2000.d01-9.x.

Anderson, L.G., Falck, E., Jones, E.P., Jutterström, S., Swift, J.H., 2004. Enhanced uptake of atmospheric $CO_2$ during freezing of seawater: a field study in Storfjorden, Svalbard. J. Geophys. Res. 109 (C6), C06004, http://dx.doi.org/10.1029/2003JC002120.

Anderson, L.G., Tanhua, T., Björk, G., Hjalmarsson, S., Jones, E.P., Jutterström, S., Rudels, B., Swift, J.H., Wåhlström, I., 2010. Arctic Ocean shelf-basin interaction: an active continental shelf $CO_2$ pump and its impact on the degree of calcium carbonate solubility. Deep-Sea Res. I 57 (7), 869–879, http://dx.doi.org/10.1016/j.dsr.2010.03.012.

Anderson, L.G., Andersson, P.S., Björk, G., Peter Jones, E., Jutterström, S., Wåhlström, I., 2013. Source and formation of the upper halocline of the arctic ocean. J. Geophys. Res.: Oceans 118 (1), 410–421, http://dx.doi.org/10.1029/2012JC008291.

Arrigo, K.R., van Dijken, G., Pabi, S., 2008. Impact of a shrinking Arctic ice cover on marine primary production. Geophys. Res. Lett. 35 (19), L19603, http://dx.doi.org/10.1029/2008GL035028.

Arrigo, K.R., Pabi, S., van Dijken, G.L., Maslowski, W., 2010. Air-sea flux of $CO_2$ in the Arctic Ocean, 1998–2003. J. Geophys. Res. 115, G04024, http://dx.doi.org/10.1029/2009JG001224.

Azetsu-Scott, K., Clarke, A., Falkner, K., Hamilton, J., Jones, E.P., Lee, C., Petrie, B., Prinsenberg, S., Starr, M., Yeats, P., 2010. Calcium carbonate saturation states in the waters of the Canadian Arctic Archipelago and the Labrador Sea. J. Geophys. Res. 115, C11021, http://dx.doi.org/10.1029/2009JC005917.

Azetsu-Scott, K., Petrie, B., Yeats, P., Lee, C., 2012. Composition and fluxes of freshwater through Davis Strait using multiple chemical tracers. J. Geophys. Res.: Oceans 117 (C12), C12011, http://dx.doi.org/10.1029/2012JC008172.

Bates, N., Grebmeier, J., Cooper, L., 2007. Healy 32H120020718, SBI Summer cruise data from the 2002 cruises, CARINA data set. Technical report, Carbon Dioxide Information Analysis Center, Oak Ridge National Laboratory, Department of Energy, Oak Ridge, Tennessee, US, http://dx.doi.org/10.3334/CDIAC/otg.CARINA_32H120020718.

Bates, N.R., Mathis, J.T., 2009. The Arctic Ocean marine carbon cycle: evaluation of air-sea $CO_2$ exchanges, ocean acidification impacts and potential feedbacks. Biogeosciences 6 (11), 2433–2459.

Bates, N.R., Moran, S.B., Hansell, D.A., Mathis, J.T., 2006. An increasing $CO_2$ sink in the Arctic Ocean due to sea-ice loss. Geophys. Res. Lett. 33 (23), 1–77.

Bellerby, R.G.J., Smethie, W.M., 2007. Knorr 316N20020530 (Nordic '02, NS02, KN166_11) cruise data from the 2002 cruises, CARINA data set. Technical Report, Carbon Dioxide Information Analysis Center, Oak Ridge National Laboratory, Department of Energy, Oak Ridge, Tennessee, US, http://dx.doi.org/10.3334/CDIAC/otg.CARINA_316N20020530.

Brown, Z.W., Arrigo, K.R., 2012. Contrasting trends in sea ice and primary production in the Bering Sea and Arctic Ocean. ICES J. Mar. Sci.: J. Cons. 69 (7), 1180–1193.

Cai, W.-J., Chen, L., Chen, B., Gao, Z., Lee, S.H., Chen, J., Pierrot, D., Sullivan, K., Wang, Y., Hu, X., Huang, W.-J., Zhang, Y., Xu, S., Murata, A., Grebmeier, J.M., Jones, E.P., Zhang, H., 2010. Decrease in the $CO_2$ uptake capacity in an ice-free Arctic Ocean basin. Science 329 (5991), 556–559, http://dx.doi.org/10.1126/science.1189338.

Carmack, E., Wassmann, P., 2006. Food webs and physical-biological coupling on pan-arctic shelves: unifying concepts and comprehensive perspectives. Progr. Oceanogr. 71 (2–4), 446–477, http://dx.doi.org/10.1016/j.pocean.2006.10.004.

Chierici, M., Fransson, A., 2009. Calcium carbonate saturation in the surface water of the Arctic Ocean: undersaturation in freshwater influenced shelves. Biogeosciences 6 (11), 2421–2431.

Codispoti, L., Swift, J., 2007. Healy 32H120040718, SBI cruise data from the 2004 cruises, CARINA data set. Technical Report, Carbon Dioxide Information Analysis Center, Oak Ridge National Laboratory, Department of Energy, Oak Ridge, Tennessee, US, http://dx.doi.org/10.3334/CDIAC/otg.CARINA_32H120040718.

Dittmar, T., Kattner, G., 2003. The biogeochemistry of the river and shelf ecosystem of the Arctic Ocean: a review. Mar. Chem. 83, 103–120, http://dx.doi.org/10.1016/S0304-4203(03)00105-1.

Else, B., Papakyriakou, T., Asplin, M., Barber, D., Galley, R., Miller, L., Mucci, A., 2013a. Annual cycle of air–sea $CO_2$ exchange in an Arctic polynya region. Glob. Biogeochem. Cycles 27, http://dx.doi.org/10.1002/gbc.20016.

Else, B.G.T., Galley, R.J., Lansard, B., Barber, D.G., Brown, K., Miller, L.A., Mucci, A., Papakyriakou, T.N., Tremblay, J.É., Rysgaard, S., 2013b. Further observations of a decreasing atmospheric $CO_2$ uptake capacity in the Canada Basin (Arctic Ocean) due to sea ice loss. Geophys. Res. Lett. 40 (6), 1132–1137, http://dx.doi.org/10.1002/grl.50268.

Else, B.G.T., Papakyriakou, T.N., Galley, R.J., Drennan, W.M., Miller, L.A., Thomas, H., 2011. Wintertime $CO_2$ fluxes in an Arctic polynya using eddy covariance: evidence for enhanced air-sea gas transfer during ice formation. J. Geophys. Res. 116, C00G03, http://dx.doi.org/10.1029/2010JC006760.

Fahrbach, E., Lemke, P., 2005. The expedition ARKTIS-XXI/1 a and b of the Research Vessel "Polarstern" in 2005, in ARK-XX/2. Cruise report, Alfred-Wegener Institute, Germany.

Falck, E., Olsen, A., 2010. Nordic Seas dissolved oxygen data in CARINA. Earth Syst. Sci. Data 2 (1), 123–131, http://dx.doi.org/10.5194/essd-2-123-2010.

Fransson, A., Chierici, M., Anderson, L.C., Bussmann, I., Kattner, G., Jones, E.P., Swift, J.H., 2001. The importance of shelf processes for the modification of chemical constituents in the waters of the Eurasian Arctic Ocean: implication for carbon fluxes. Cont. Shelf Res. 21 (3), 225–242, http://dx.doi.org/10.1016/S0278-4343(00)00088-1.

Fransson, A., Chierici, M., Nojiri, Y., 2009. New insights into the spatial variability of the surface water carbon dioxide in varying sea ice conditions in the Arctic Ocean. Cont. Shelf Res. 29 (10), 1317–1328, http://dx.doi.org/10.1016/j.csr.2009.03.008.

Garneau, M.E., Gosselin, M., Klein, B., Tremblay, J.E., Fouilland, E., 2007. New and regenerated production during a late summer bloom in an Arctic polynya. Mar. Ecol. Progr. Ser. 345, 13–26, http://dx.doi.org/10.3354/meps06965.

Gruber, N., Gloor, M., Mikaloff Fletcher, S.E., Doney, S.C., Dutkiewicz, S., Follows, M. J., Gerber, M., Jacobson, A.R., Joos, F., Lindsay, K., Menemenlis, D., Mouchet, A., Müller, S.A., Sarmiento, J.L., Takahashi, T., 2009. Oceanic sources sinks and transport of atmospheric $CO_2$. Glob. Biogeochem. Cycles 23 (1), GB1005, http://dx.doi.org/10.1029/2008GB003349.

Hansell, D.A., Kadko, D., Bates, N.R., 2004. Degradation of terrigenous dissolved organic carbon in the western Arctic Ocean. Science 304 (5672), 858–861, http://dx.doi.org/10.1126/science.1096175.

Holmes, R.M., McClelland, J.W., Peterson, B.J., Tank, S.E., Bulygina, E., Eglinton, T.I., Gordeev, V.V., Gurtovaya, T.Y., Raymond, P.A., Repeta, D.J., Staples, R., Striegl, R. G., Zhulidov, A.V., Zimov, S.A., 2012. Seasonal and annual fluxes of nutrients and organic matter from large rivers to the Arctic Ocean and surrounding seas. Estuar. Coasts 35, 369–382, http://dx.doi.org/10.1007/s12237-011-9386-6.

Ito, T., Follows, M.J., Boyle, E.A., 2004. Is AOU a good measure of respiration in the oceans? Geophys. Res. Lett. 31 (17), L17305, http://dx.doi.org/10.1029/2004GL020900.

Jahn, A., Tremblay, L.B., Newton, R., Holland, M.M., Mysak, L.A., Dmitrenko, I.A., 2010. A tracer study of the Arctic Ocean's liquid freshwater export variability. J. Geophys. Res.: Oceans 115 (C7), C07015, http://dx.doi.org/10.1029/2009JC005873.

Jeansson, E., Olsen, A., Eldevik, T., Skjelvan, I., Omar, A.M., Lauvset, S.K., Nilsen, J.E.Ø., Bellerby, R.G.J., Johannessen, T., Falck, E., 2011. The Nordic Seas carbon budget: sources, sinks, and uncertainties. Glob. Biogeochem. Cycles 25 (4), GB4010, http://dx.doi.org/10.1029/2010GB003961.

Johannessen, T., Olsen, A., 2007. G.o. sars 58gs20030922 cruise data from the 2003 cruises, carina data set. Technical Report, Carbon Dioxide Information Analysis Center, Oak Ridge National Laboratory, Department of Energy, Oak Ridge, Tennessee, US, http://dx.doi.org/10.3334/CDIAC/otg.CARINA_58GS20030922.

Jones, P., Azetsu-Scott, K., MacLaughlin, F.A., Falkner, K., 2007. L.S. St-Laurent 18SNA097 (Expocode: 18SN19970803), JOIS 97, Leg 1 cruise data from the 1997 cruises, CARINA data set. Technical Report, Carbon Dioxide Information Analysis Center, Oak Ridge National Laboratory, Department of Energy, Oak Ridge, Tennessee, US, http://dx.doi.org/10.3334/CDIAC/otg.CARINA_18SN19970803.

Jutterström, S., Anderson, L.G., 2010. Uptake of $CO_2$ by the Arctic Ocean in a changing climate. Mar. Chem. 122 (1–4), 96–104, http://dx.doi.org/10.1016/j.marchem.2010.07.002.

Jutterström, S., Anderson, L.G., Bates, N.R., Bellerby, R.G.J., Johannessen, T., Jones, E. P., Key, R.M., Lin, X., Olsen, A., Omar, A.M., 2010. Arctic Ocean data in CARINA. Earth Syst. Sci. Data 2, 71–78.

Kaltin, S., Anderson, L.G., 2005. Uptake of atmospheric carbon dioxide in Arctic shelf seas: evaluation of the relative importance of processes that influence $pCO_2$ in water transported over the Bering-Chukchi Sea shelf. Mar. Chem. 94 (1–4), 67–79, http://dx.doi.org/10.1016/j.marchem.2004.07.010.

Kaltin, S., Anderson, L.G., Olsson, K., Fransson, A., Chierici, M., 2002. Uptake of atmospheric carbon dioxide in the Barents Sea. J. Mar. Syst. 38 (1–2), 31–45, http://dx.doi.org/10.1016/S0924-7963(02)00168-9.

Khatiwala, S., Primeau, F., Hall, T., 2009. Reconstruction of the history of anthropogenic $CO_2$ concentrations in the ocean. Nature 462 (7271), 346–350, http://dx.doi.org/10.1038/nature08526.

Kivimae, C., Bellerby, R.G.J., Fransson, A., Reigstad, M., Johannessen, T., 2010. A carbon budget for the Barents Sea. Deep-Sea Res. I 57 (12), 1532–1542, http://dx.doi.org/10.1016/j.dsr.2010.05.006.

Lalande, C., Bélanger, S., Fortier, L., 2009a. Impact of a decreasing sea ice cover on the vertical export of particulate organic carbon in the northern Laptev Sea, Siberian Arctic Ocean. Geophys. Res. Lett. 36, L21604, http://dx.doi.org/10.1029/2009GL040570.

Lalande, C., Forest, A., Barber, D.G., Gratton, Y., Fortier, L., 2009b. Variability in the annual cycle of vertical particulate organic carbon export on Arctic shelves: contrasting the Laptev Sea, Northern Baffin Bay and the Beaufort sea. Cont. Shelf Res. 29 (17), 2157–2165, http://dx.doi.org/10.1016/j.csr.2009.08.009.

Lee, C.M., Abriel, J., Gabat, J.I., Petrie, B., Scotney, M., Soukhovtsev, V., Thiel, K.V., 2004. An observational array for high-resolution, year-round measurements of volume, freshwater, and ice flux variability in Davis Strait: Cruise report for R/V Knorr 179–05, 22 September–4 October 2004. Report, University of Washington, Seattle, Washington.

Letscher, R.T., Hansell, D.A., Kadko, D., 2011. Rapid removal of terrigenous dissolved organic carbon over the Eurasian shelves of the Arctic Ocean. Mar. Chem. 123 (1–4), 78–87, http://dx.doi.org/10.1016/j.marchem.2010.10.002.

Lundberg, L., Haugan, P.H., 1996. A Nordic Seas-Arctic Ocean carbon budget from volume flows and inorganic carbon data. Glob. Biogeochem. Cycles 10 (3), 493–510.

MacDonald, R.W., Anderson, L.G., Christensen, J., Miller, L.A., Semiletov, I.P., Stein, R., 2010. The Arctic Ocean. In: Liu, K.-K., Atkinson, L., Quinones, R., Talaue-McManus, L. (Eds.), Carbon and Nutrient Fluxes in Continental Margins: A Global Synthesis. Springer-Verlag, Berlin, pp. 289–303

Manizza, M., Follows, M.J., Dutkiewicz, S., Menemenlis, D., McClelland, J.W., Hill, C. N., Peterson, B.J., Key, R.M., 2011. A model of the Arctic Ocean carbon cycle. J. Geophys. Res. 116, C12020, http://dx.doi.org/10.1029/2011JC006998.

Manizza, M., Follows, M.J., Dutkiewicz, S., Menemenlis, D., Hill, C.N., Key, R.M., 2013. Changes in the Arctic Ocean $CO_2$ sink (1996–2007): a regional model analysis. Glob. Biogeochem. Cycles , http://dx.doi.org/10.1002/2012GB004491

Marnela, M., Rudels, B., Olsson, K.A., Anderson, L.G., Jeansson, E., Torres, D.J., Messias, M.-J., Swift, J.H., Watson, A.J., 2008. Transports of Nordic Seas water

masses and excess SF6 through Fram Strait to the Arctic Ocean. Progr. Oceanogr. 78 (1), 1–11 http://dx.doi.org/10.1016/j.pocean.2007.06.004.
Mathis, J.T., Pickart, R.S., Byrne, R.H., McNeil, C.L., Moore, G.W.K., Juranek, L.W., Liu, X.W., Ma, J., Easley, R.A., Elliot, M.M., Cross, J.N., Reisdorph, S.C., Bahr, F., Morison, J., Lichendorf, T., Feely, R.A., 2012. Storm-induced upwelling of high $pCO_2$ waters onto the continental shelf of the western Arctic Ocean and implications for carbonate mineral saturation states. Geophys. Res. Lett. 39, L07606, http://dx.doi.org/10.1029/2012GL051574.
McGuire, A.D., Anderson, L.G., Christensen, T.R., Dallimore, S., Guo, L.D., Hayes, D.J., Heimann, M., Lorenson, T.D., MacDonald, R.W., Roulet, N., 2009. Sensitivity of the carbon cycle in the Arctic to climate change. Ecol. Monogr. 79 (4), 523–555, http://dx.doi.org/10.1890/08-2025.1.
Michel, C., Gosselin, M., Nozais, C., 2002. Preferential sinking export of biogenic silica during the spring and summer in the North Water polynya (northern Baffin Bay): temperature or biological control?. J. Geophys. Res. 107 (C7), http://dx.doi.org/10.1029/2000JC000408.
Murata, A., Takizawa, T., 2003. Summertime $CO_2$ sinks in shelf and slope waters of the western Arctic Ocean. Cont. Shelf Res. 23, 753–776.
Olsen, A., Omar, A.M., Jeansson, E., Anderson, L.G., Bellerby, R.G.J., 2010. Nordic seas transit time distributions and anthropogenic $CO_2$. J. Geophys. Res. 115 (C5), C05005, http://dx.doi.org/10.1029/2009JC005488.
Pabi, S., vanDijken, G.L., Arrigo, K.R., 2008. Primary production in the Arctic Ocean, 1998–2006. J. Geophys. Res.: Oceans 113 (C8), C08005, http://dx.doi.org/10.1029/2007JC004578.
Perrette, M., Yool, A., Quartly, G.D., Popova, E.E., 2011. Near-ubiquity of ice-edge blooms in the Arctic. Biogeosciences 8 (2), 515–524, http://dx.doi.org/10.5194/bg-8-515-2011.
Rabe, B., Schauer, U., Mackensen, A., Karcher, M.J., Hansen, E., Beszczynska-Möller, A., 2009. Freshwater components and transports in the Fram Strait—recent observations and changes since the late 1990s. Ocean Sci. 5 (3), 219–233.
Rachold, V., Eicken, H., Gordeev, V.V., Grigoriev, M.N., Hubberten, H.W., Lisitzin, A.P., Shevchenko, V., Schirrmeister, L., 2004. Modern terrigenous organic carbon input to the Arctic Ocean. In: Stein, R., Macdonald, R.W. (Eds.), The Organic Carbon Cycle in the Arctic Ocean. Springer, Berlin, pp. 33–55
Raymond, P.A., McClelland, J.W., Holmes, R.M., Zhulidov, A.V., Mull, K., Peterson, B.J., Striegl, R.G., Aiken, G.R., Gurtovaya, T.Y., 2007. Flux and age of dissolved organic carbon exported to the Arctic Ocean: a carbon isotopic study of the five largest arctic rivers. Glob. Biogeochem. Cycles 21 (4), GB4011, http://dx.doi.org/10.1029/2007GB002934.
Roemmich, D., 1983. Optimal estimation of hydrographic station data and derived fields. J. Phys. Oceanogr. 13 (8), 1544–1549, http://dx.doi.org/10.1175/1520-0485(1983)013<1544:OEOHSD>2.0.CO;2.
Rudels, B., 1987. On the mass balance of the polar ocean, with special emphasis on the Fram Strait. Norsk Polarinstitutt Skrifter 188, 53.
Rudels, B., Bjork, G., Nilsson, J., Winsor, P., Lake, I., Nohr, C., 2005. The interaction between waters from the Arctic Ocean and the Nordic Seas north of Fram Strait and along the East Greenland Current: results from the Arctic Ocean-02 Oden expedition. J. Mar. Syst. 55 (1–2), 1–30, http://dx.doi.org/10.1016/j.jmarsys.2004.06.008.
Rysgaard, S., Glud, R.N., Sejr, M.K., Bendtsen, J., Christensen, P.B., 2007. Inorganic carbon transport during sea ice growth and decay: a carbon pump in polar seas. J. Geophys. Res. 112 (C3), C03016, http://dx.doi.org/10.1029/2006JC003572.
Rysgaard, S., Bendtsen, J., Delille, B., Dieckmann, G.S., Glud, R.N., Kennedy, H., Mortensen, J., Papadimitriou, S., Thomas, D.N., Tison, J.L., 2011. Sea ice contribution to the air-sea $CO_2$ exchange in the Arctic and Southern Oceans. Tellus Ser. B 63 (5), 823–830, http://dx.doi.org/10.1111/j.1600-0889.2011.00571.x.
Sabine, C.L., Feely, R.A., Gruber, N., Key, R.M., Lee, K., Bullister, J.L., Wanninkhof, R., Wong, C.S., Wallace, D.W.R., Tilbrook, B., Millero, F.J., Peng, T.-H., Kozyr, A., Ono, T., Rios, A.F., 2004. The oceanic sink for anthropogenic $CO_2$. Science 305 (5682), 367–371, http://dx.doi.org/10.1126/science.1097403.
Sarmiento, J.L., Gruber, N., 2006. Ocean Biogeochemical Dynamics, first edition Princeton University Press, Princeton
Schlosser, P., Swift, J.H., Lewis, D., Pfirman, S.L., 1995. The role of the large-scale Arctic Ocean circulation in the transport of contaminants. Deep-Sea Res. II 42 (6), 1341–1367.
Schmidt, G.A., Bigg, G.R., Rohling, E.J., 1999. Global seawater oxygen-18 database—v1.21. Report, ⟨http://data.giss.nasa.gov/o18data/⟩.
Schuster, U., McKinley, G.A., Bates, N., Chevallier, F., Doney, S.C., Fay, A.R., Gonzalez-Davila, M., Gruber, N., Jones, S., Krijnen, J., Landschutzer, P., Lefevre, N., Manizza, M., Mathis, J., Metzl, N., Olsen, A., Rios, A.F., Rodenbeck, C., Santana-Casiano, J.M., Takahashi, T., Wanninkhof, R., Watson, A.J., 2013. An assessment of the Atlantic and Arctic sea-air $CO_2$ fluxes, 1990–2009. Biogeosciences 10 (1), 607–627, http://dx.doi.org/10.5194/bg-10-607-2013.
Shadwick, E.H., Thomas, H., Gratton, Y., Leong, D., Moore, S.A., Papakyriakou, T., Prowe, A.E.F., 2011. Export of Pacific carbon through the Arctic Archipelago to the North Atlantic. Cont. Shelf Res. 31 (7–8), 806–816, http://dx.doi.org/10.1016/j.csr.2011.01.014.
Skagseth, O., Furevik, T., Ingvaldsen, R., Loeng, H., Mork, K., Orvik, K., Ozhigin, V., 2008. Volume and heat transports to the Arctic Ocean via the Norwegian and Barents seas. In: Dickson, R.R., Meincke, J., Rhines, P. (Eds.), Arctic-Subarctic Ocean Fluxes: Defining the Role of the Northern Seas in Climate. Springer, Dordrecht, Netherlands, pp. 45–64
Skjelvan, I., Falck, E., Rey, F., Kringstad, S.B., 2008. Inorganic carbon time series at Ocean Weather Station M in the Norwegian Sea. Biogeosciences 5 (2), 549–560.
Takahashi, T., Sutherland, S.C., Wanninkhof, R., Sweeney, C., Feely, R.A., Chipman, D.W., Hales, B., Friederich, G., Chavez, F., Sabine, C., Watson, A., Bakker, D.C., Schuster, U., Metzl, N., Yoshikawa-Inoue, H., Ishii, M., Midorikawa, T., Nojiri, Y., Körtzinger, A., Steinhoff, T., Hoppema, M., Olafsson, J., Arnarson, T.S., Tilbrook, B., Johannessen, T., Olsen, A., Bellerby, R., Wong, C., Delille, B., Bates, N., de Baar, H.J., 2009. Climatological mean and decadal change in surface ocean $pCO_2$, and net sea–air $CO_2$ flux over the global oceans. Deep Sea Res. Part II 56 (8–10), 554–577, http://dx.doi.org/10.1016/j.dsr2.2008.12.009.
Tang, C.C.L., Ross, C.K., Yao, T., Petrie, B., DeTracey, B.M., Dunlap, E., 2004. The circulation, water masses and sea-ice of Baffin Bay. Progr. Oceanogr. 63 (4), 183–228, http://dx.doi.org/10.1016/j.pocean.2004.09.005.
Tanhua, T., Jones, E.P., Jeansson, E., Jutterström, S., Smethie, W.M., Wallace, D.W.R., Anderson, L.G., 2009. Ventilation of the Arctic Ocean: mean ages and inventories of anthropogenic $CO_2$ and CFC-11. J. Geophys. Res. 114 (C1), C01002, http://dx.doi.org/10.1029/2008JC004868.
Tank, S.E., Raymond, P.A., Striegl, R.G., McClelland, J.W., Holmes, R.M., Fiske, G.J., Peterson, B.J., 2012. A land-to-ocean perspective on the magnitude, source and implication of DIC flux from major Arctic rivers to the Arctic Ocean. Glob. Biogeochem. Cycles 26 (4), GB4018, http://dx.doi.org/10.1029/2011GB004192.
Toole, J.M., Timmermans, M.L., Perovich, D.K., Krishfield, R.A., Proshutinsky, A., Richter-Menge, J.A., 2010. Influences of the ocean surface mixed layer and thermohaline stratification on Arctic Sea ice in the central Canada Basin. J. Geophys. Res. 115, C10018, http://dx.doi.org/10.1029/2009JC005660.
Torres-Valdés, S., Tsubouchi, T., Bacon, S., Naveira-Garabato, A.C., Sanders, R., McLaughlin, F.A., Petrie, B., Kattner, G., Azetsu-Scott, K., Whitledge, T.E., 2013. Export of nutrients from the arctic ocean. J. Geophys. Res.: Oceans 118, http://dx.doi.org/10.1002/jgrc.20063.
Tremblay, J.-É., Gratton, Y., Carmack, E.C., Payne, C.D., Price, N.M., 2002. Impact of the large-scale Arctic circulation and the North Water Polynya on nutrient inventories in Baffin Bay. J. Geophys. Res. 107 (C8), 26-1–26-14, http://dx.doi.org/10.1029/2000JC000595.
Tsubouchi, T., Bacon, S., Garabato, A.C.N., Aksenov, Y., Laxon, S.W., Fahrbach, E., Beszczynska-Moller, A., Hansen, E., Lee, C.M., Ingvaldsen, R.B., 2012. The Arctic Ocean in summer: a quasi-synoptic inverse estimate of boundary fluxes and water mass transformation. J. Geophys. Res. 117, C01024, http://dx.doi.org/10.1029/2011JC007174.
van Heuven, S., Pierrot, D., Lewis, E., Wallace, D.W.R., 2009. Matlab program developed for $CO_2$ system calculations, ornl/cdiac-105b. Technical Report, Carbon Dioxide Information Analysis Center, Oak Ridge National Laboratory, Department of Energy, Oak Ridge, Tennessee, US.
Williams, R.G., Follows, M.J., 2011. Ocean Dynamics and the Carbon Cycle: Principles and Mechanisms, first edition Cambridge University Press, Cambridge
Woodgate, R.A., Weingartner, T.J., Whitledge, T.E., Lindsay, R., Crane, K., 2008. The Pacific gateway to the Arctic–Quantifying and understanding Bering Strait oceanic fluxes. Russian American Long-term census of the Arctic. Report, NOAA, Silver Spring, Maryland.
Yamamoto-Kawai, M., Tanaka, N., 2005. Freshwater and brine behaviors in the Arctic Ocean deduced from historical data of $\delta^{18}O$ and alkalinity (1929–2002 A.D.). J. Geophys. Res. 110, C10003, http://dx.doi.org/10.1029/2004JC002793.